ORIGINAL RESEARCH

Seasonality in commodity prices: new approaches for pricing plain vanilla options

Carme Frau[1] · Viviana Fanelli[2]

Abstract
We present a new term-structure model for commodity futures prices based on Trolle and Schwartz (2009), which we extend by incorporating seasonal stochastic volatility represented with two different sinusoidal expressions. We obtain a quasi-analytical representation of the characteristic function of the futures log-prices and closed-form expressions for standard European options' prices using the fast Fourier transform algorithm. We price plain vanilla options on the Henry Hub natural gas futures contracts, using our model and extant models. We obtain higher accuracy levels with our model than with the extant models.

Keywords Commodities · Natural gas · Futures prices · Option pricing · Fast Fourier transform · Term-structure model · Analytical solution · Seasonal stochastic volatility · Sinusoidal functions

JEL Classification C51 · C63 · G13

✉ Carme Frau
carme.frau@uib.es
https://personal.uib.es/carme.frau

Viviana Fanelli
viviana.fanelli@uniba.it
https://www.uniba.it/docenti/fanelli-viviana

[1] Department of Business Economics, Universitat de les Illes Balears, Ctra. de Valldemossa km 7.5, 07122 Palma de Mallorca, Spain

[2] Department of Economics, Management and Business Law, Largo Abbazia Santa Scolastica 53, 70124 Bari, Italy

1 Introduction

In this paper we aim at finding a suitable model for pricing commodities in the spot and futures markets, which are characterised by stochastic prices and cost of carry, and seasonal stochastic volatility (**SSV** hereafter). In this perspective, we review a great deal of literature on spot and futures models. In Table 1 we list the models for spot and futures prices we comment in this section in order to get a meaningful framework of the existing models and highlight the gap in the literature we fill with our work. Within it, we indicate what stochastic factors, volatility type and jumps they present, the number of parameters included and, in the case of commodity assets, the underlyings in the empirical analysis. In addition, we reference Fanelli (2020) to provide a concise survey of arbitrage pricing models for commodities.

The next classical models evolve from displaying Gaussian to non-Gaussian returns in different ways. In Black and Scholes (1973) (**BS73** hereafter) the spot price is modeled through a geometric Brownian motion. Merton (1976) (**Mer76** hereafter) defines the spot dynamics by using a stochastic process which includes iid jumps. Heston (1993) (**Hes93** hereafter) proposes a model with stochastic volatility for pricing contracts on spot prices. And Bates (1996) (**Bat96** hereafter) uses a combination of stochastic volatility and jump-diffusion processes for modeling spot prices when jump and volatility risks are systematic and non-diversifiable. The empirical analysis performed in these models relies on equity or FX underlying assets.

The following theoretical models propose a time-damping structure to the volatility functions. Clewlow and Strickland (1999) (**CS99b** hereafter) propose a one-factor model with a time-decaying volatility of the forward prices using two parameters, and Clewlow and Strickland (1999) (**CS99a** hereafter) proposes the correspondent multi-dimensional model to CS99b. The main strength of CS99a is that it develops a framework consistent with the market observable forward price curve as well as with the volatilities and correlations of forward prices. Clewlow and Strickland (2000) (**CS00** hereafter) add a long-term volatility parameter to the latter.

In the remaining of this section, we present models which study different types of commodities. Eydeland and Geman (1998) (**EG98** hereafter) and Geman (2000) (**Gem00** hereafter) propose similar models for spot prices which are a mean-reverting extension of the Hes93 model; the former focuses on electricity and natural gas, the latter on crude oil. Under the risk-neutral probability measure, Lucia and Schwartz (2002) (**LS02** hereafter) propose one- and two-factor models for electricity spot prices, and then a sinusoidal function to capture the seasonal behaviour of the futures curve directly implied in the spot price dynamics.

In Sørensen (2002) (**Sor02** hereafter), agricultural commodity prices are modeled as a sum of a deterministic seasonal component, a non-stationary state-variable, and a stationary state-variable. Futures prices are established by standard no-arbitrage arguments. Richter and Sørensen (2002) (**RS02** hereafter) estimate a continuous-time stochastic volatility model for agricultural spot prices, reflecting seasonality patterns in both the spot price and the volatility. Geman and Nguyen (2005) (**GN05** hereafter) assume that agricultural spot prices are the sum of two components: one being seasonal and deterministic and the other stochastic and mean-reverting. By developing these two- and three-state variable models, futures prices are obtained through the classical spot-forward price relationship.

Trolle and Schwartz (2009) (**TS09** hereafter) develop a parsimonious and highly tractable model for pricing commodity derivatives in the presence of unspanned stochastic volatility (**USV** hereafter). They use two factors to model the movements of the future prices under the

risk-neutral probability measure, the spot price and the forward cost of carry curve, and one or two variance factors to frame their three- and four-factor model specification, namely SV1, SV2 and SV2gen. They then obtain an affine model for futures curves and price standard American options on crude oil.

Back et al. (2013) (**BPP13** hereafter) propose one- and two-factor models for the logarithm of the spot price, which shows a seasonal pattern. In particular, the spot price is composed by two stochastic components which are mean-reverting and have seasonal volatility, and an additional seasonal component. The forward dynamics is obtained by applying the spot-forward price relationship. Their empirical analysis is performed on crude oil, natural gas and agriculturals. Arismendi et al. (2016) (**ABP16** hereafter) model agricultural and natural gas futures price under the risk-neutral measure where the instantaneous variance of futures returns is described through a mean-reverting square-root process, where the long-term parameter is seasonal and follows an exponential sinusoidal form.

Fanelli et al. (2016) (**FMM16** hereafter) considers a seasonal path-dependent volatility for electricity futures returns in the trading date, which is modeled following the Heath et al. (1992) framework, and they obtain the dynamics of futures prices. Fanelli and Schmeck (2019) (**FS19** hereafter) focuses on the seasonality found in the implied volatility of electricity option prices in the delivery period.

Santangelo (2017) (**San17** hereafter) proposes a model with mean-reversion in natural gas spot prices and stochastic jump intensity linked to the temperature. And Brix et al. (2018) (**BLW18** hereafter) incorporate spikes in a mean-reverting specification of the natural gas spot and forward prices with trend and seasonality.

More recently, Schneider and Tavin (2018) (**ST18** hereafter) propose a multi-factor stochastic volatility model for crude oil futures contracts, with an expiry-dependent volatility term which is able to capture the Samuelson volatility effect. Schneider and Tavin (2021) (**ST21** hereafter) extend their previous model by incorporating a seasonal mean-reverting level in the variance and study agricultural commodities; they propose five different expressions to be followed by this seasonal component (among which there is a sinusoidal and an exponential sinusoidal pattern). In this paper, we focus on the natural gas market.

Over the last few years, natural gas has become one of the most utilised energy sources worldwide, second only to oil and coal, and is expected to overtake the latter by 2030. Natural gas is used to fuel electricity power plants, as well as industrial, commercial and domestic cooking and heating. The overall trend of the natural gas price, its periodicity, volatility and related behavior, and term-structure correlation are driven by production fundamentals and relationships, demand, demand elasticity and storage.

The countries with the largest production of natural gas are currently the US, Russia, Iran, Qatar, Canada, China and Norway. All of these countries serve their domestic markets, and export excess around the world through pipelines or as liquefied natural gas. The demand for natural gas is very high in western Europe, north America and north Asia, where it is satisfied through dense pipeline networks.

The foremost global trading center is the Henry Hub (**HH** hereafter), it is strategically situated in the state of Louisiana (US), a major onshore production region and close to offshore production. It is also connected to storage facilities, interstate and intrastate pipeline systems; therefore, its production can be easily moved from supply basins and exported to major consumption markets. These features make the HH the dominant global reference price for natural gas, especially for futures contracts.

Gas production in the US is steadily increasing, while gas storage level also plays a key role when looking at supply side. During periods of lower demand, production surplus can be injected into storage facilities in the form of liquefied natural gas, which can later provide a

valuable cushion to meet demand peaks. However, liquefied natural gas storage can be utilised to meet sudden demand increase or decrease only up to a point. Natural gas supply is always affected by a relatively wide range of prices. Restrictions in the existing gas infrastructure impact additional flows, rendering the supply curve very inelastic when prices are high.

Overall economic growth, weather and competing fuel prices are also significant factors in natural gas demand. Major demand-side players include: (i) industrial organisations which use it to produce electricity due to its low price relative to coal, and as raw material to produce fertilisers, chemicals and hydrogen; (ii) transportation consumers using liquefied natural gas as vehicle fuel; (iii) industrial, commercial and domestic consumers using it as fuel for heating and in some cases cooling.

Weather is the main factor in natural gas price evolution, leading to seasonal price behaviour and stochastic volatility. During the northern hemisphere's fall and winter seasons, gas prices are higher due to increased demand for heating, and it is very volatile. In northern spring and summer, gas demand decreases, but production continues, as excess can be stored as liquefied natural gas, thus exhibiting less variability during this period. Considering the cyclical behaviour of natural gas prices is key to predict winter demand; therefore winter futures typically trade at a premium compared to summer ones. Understanding the seasonality in natural gas markets and the potential impact on its prices is useful for researchers and practitioners in the field of trading strategies.

The stylised facts in the natural gas market are mean-reversion and jumps in prices, seasonality in prices and in implied volatilities, the inverse leverage effect (**ILE** hereafter) and the Samuelson effect; they are all described in detail in Sect. 3.2. In the literature, among papers which focus on the modeling of natural gas prices, we recall EG98, BPP13, ABP16, San17 and BLW18. Seasonal (stochastic) volatility is a well-known empirical feature for many commodities in the literature, specially agriculturals and natural gas. Therefore, the framework we present goes beyond a particular asset, natural gas, and our model is extendable to other commodities driven by seasonality factors, such as agriculturals.

We propose a three-factor model which we refer to as **SYSSV**[1] for futures prices with three stochastic factors: the spot price, the cost of carry curve and the instantaneous variance. The variance follows a mean-reverting square-root process which incorporates the seasonality in its long-run mean-reversion level. We obtain the futures prices in the original framework and also propose an alternative characterisation or set-up of the parameters. We price standard European options on HH natural gas futures contracts, with maturities ranging from approximately one to two months up to 1 year. Our benchmark model is the three-factor version of TS09 (**TS09-SV1** hereafter), which on average we outperform slightly. However, a more granular analysis evidences that our model clearly outperforms the benchmark for short maturities and deep OTM (ATM and close to the ATM) options under the original (alternative) set-up. An additional benefit provided by the alternative set-up is that the calibration is much quicker.

The remainder of this article is structured as follows: in Sect. 2 we present a novel model formulation based on the USV model of TS09-SV1 which we extend by introducing seasonality in the variance, we derive the correspondent characteristic function of the futures prices with which we price standard European options; in Sect. 3 we describe the market data, the stylised facts, and how we perform the parameter estimation; in Sect. 4 we comment our model's results and those of other extant ones that are well known in the literature; and in Sect. 5 we present our conclusions and indicate future lines of research.

---

[1] SYSSV stands for Stochastic cost of carry curve $Y(t, T)$ and Seasonal Stochastic Volatility v_t.

Table 1 Factors and features per model

| Model	Dim. S	M	Stochastic factors S_t	$y(t,T)$	$F(t,T)$	v_t	Seasonality Price	Vols.	SSV	Jumps Price	Param. Count	Cmdty. Asset
BS73	✓		✓								1	–
Mer76	✓		✓							✓	4	–
Hes93	✓		✓			✓					4	–
Bat96	✓		✓			✓				✓	7	–
EG98	✓		✓			✓					6	G,E
Gem00	✓		✓			✓					7	O
CS99a		✓			✓						2	–
CS99b	✓				✓						2	–
CS00	✓				✓						3	–
LS02	✓		✓					✓			13	E
Sor02	✓		✓				✓				6	A
RS02	✓		✓			✓	✓	✓	✓		10	A
GN05	✓		✓			✓	✓	✓	✓		17	A
TS09-SV1	✓		✓	✓	★	✓					9(7)	O
BPP13	✓		✓				✓	✓			7,8	O,G,A
ABP16	✓				✓	✓		✓	✓		5	G,A
FMM16	✓				✓			✓			36	E
San17	✓					✓			✓		19	G
BLW18	✓		✓			✓	✓			✓	11	G
FS19	✓				✓			✓	✓		15	E
ST18		✓			✓	✓					5	O
ST21		✓			✓	✓		✓	✓		6	A
SYSSV	✓		✓	✓	★	✓		✓	✓		10,11(8,9)	G

For each model mentioned in Sect. 1, this table enumerates the factors considered, the type of seasonality, the jumps and the parameter count. Column Dim. accounts for the dimensional setting of the model (S for single, M for multiple). The acronyms whereby we refer to the models can be found in Sect. 1. In those models presenting alternative characterisation of the parameters (as defined in Sect. 2.1.2) and in the columns for the stochastic factors, $F(t,T)$ replaces S_t and $y(t,T)$; this is indicated with the symbol ★ and the correspondent parameter count appears in brackets. The commodity assets on which the articles perform their applied exercise are indicated by the following acronyms: A refers to agriculturals, E to electricity, G to natural gas, O to oil (crude or heating). The parameter count for GN05 corresponds to its two-state variable model; for LS02 corresponds to its one factor model. We refer to our model as SYSSV

2 A new three-factor model for futures prices on commodities

In this work we derive a futures-based model which can exactly match any given futures curve by specifying the futures initial values without incorporating any of the other model parameters. It fits the initial futures curve by construction, which means that the seasonality in prices is already incorporated as can be observed in Fig. 1a. Moreover, our model is term-structured, presenting a seasonality pattern in the dynamics of the futures variance. This new element affects the option pricing but not the expression followed by the expected value of the futures prices.

In this section we formalise the dynamics of the futures prices in our novel model specification, compute the corresponding characteristic function, and indicate the technical conditions

(a) Futures prices

(b) Futures volatilities
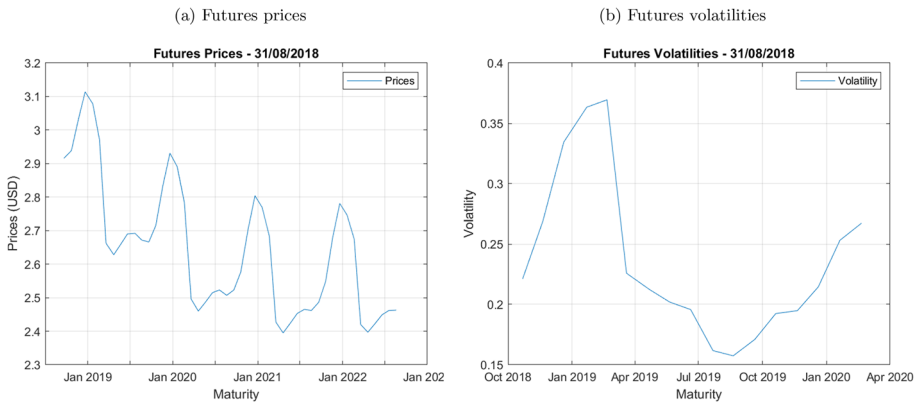
Fig. 1 Seasonality in the term-structure-31/08/2018. *Notes*: This figure presents a cross-sectional analysis of the seasonality in the natural gas market as of 31/08/2018. **a** Shows the term-structure of futures prices for contracts maturing during the following four years (M1 to M48, that is, 22/09/2018 to 20/08/2022). **b** Shows the term-structure of implied volatilities for contracts maturing during the closer months (M2 to M18, that is, 22/10/2018 to 22/02/2020). We compute implied volatilities employing the standard model of Black (1976)

under which the dynamics of the variance factor are defined. Let S_t denote the time-t spot price of the commodity, and let $y(t, T)$ denote the time-t instantaneous forward cost of carry maturing at time T, with $y(t, t) = y_t$ the time-t instantaneous spot cost of carry. We model the evolution of the entire futures curve by specifying one process for S_t and another process for $y(t, T)$. Also, let v_t denote the instantaneous variance, which follows a mean-reverting process as in Cox et al. (1985).

2.1 The model under the risk-neutral measure $\mathbb{Q}$

Consider the following three-factor model. Let $(\Omega, \mathcal{F}, \mathbb{Q})$ be a probability space on which three Brownian motion processes, W_t^S, W_t^y and W_t^v, are defined for all $0 \leq t \leq T$. Let $\mathcal{F}$ be the filtration generated by these Brownian motions. The absence of arbitrage implies the existence of a risk-neutral or equivalent martingale measure $\mathbb{Q}$ under which the processes followed by S_t, $y(t, T)$ and v_t are governed by the following dynamics

$$\frac{dS_t}{S_t} = y_t dt + \sigma_S \sqrt{v_t}\, dW_t^S, \tag{2.1}$$

$$dy(t, T) = \mu_y(t, T)dt + \sigma_y(t, T)\sqrt{v_t}\, dW_t^y, \tag{2.2}$$

$$dv_t = \kappa\,(\theta_t - v_t)\, dt + \sigma_v \sqrt{v_t}\, dW_t^v, \tag{2.3}$$

with S_t, $v_t > 0$, and allowing W_t^S, W_t^y and W_t^v to be correlated with ρ_{Sy}, ρ_{Sv} and ρ_{yv}, which denote pairwise correlations. We do not impose any type of structure to the drift term of the cost of carry curve $\mu_y(t, T)$.

This novel model formulation consists of an expansion of the three-factor model specification of TS09 (that is, TS09-SV1) with SSV. This seasonality is captured in the deterministic expression followed by θ_t, the time-varying long-run mean-reversion variance level, which particular form we address in Sect. 2.1.1. The volatility of the spot price S_t is represented by σ_S, the volatility of the variance v_t is represented by σ_v, and the volatility of the forward cost of carry curve $y(t, T)$, which we assume that follows a time-dampening form, is represented by

(a) Samuelson effect

(b) Seasonality in the variance
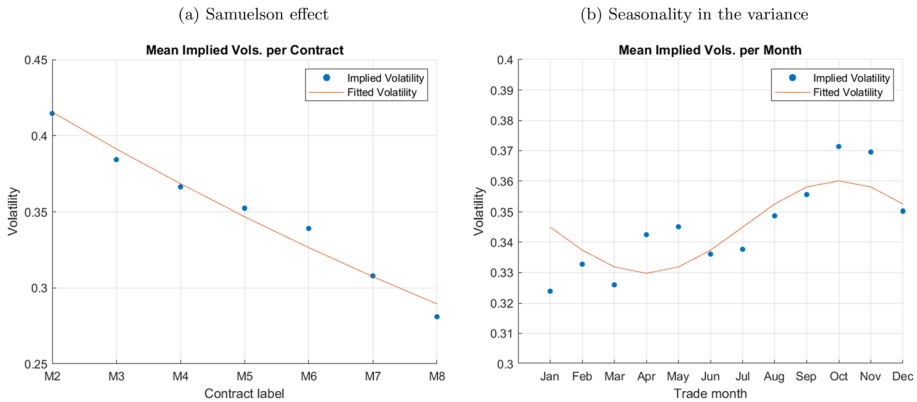
Fig. 2 Stylised facts in the variance. *Notes*: This figure presents two stylised facts in the natural gas market. **a** Shows the Samuelson effect of the implied volatilities of futures options grouped by contract (that is, from closest to maturity to more distant ones), with $R^2 = 97.19\%$. **b** Shows the seasonal pattern of the implied volatilities of futures options grouped by trade month, with $R^2 = 53.93\%$. Observe that this results is almost identical to that in Table 6c with $t_0 = 10/12$ (end of October) and single sub-specification (S). The seasonal volatility pattern is approximated by the trigonometric function following expression in (2.5). For both sub-figures, the period considered spans from 01/2011 to 12/2020 (monthly observations), and only ATM options are considered. We compute implied volatilities employing the standard model of Black (1976)

$$\sigma_y(t, T) \equiv \alpha e^{-\gamma(T-t)}, \tag{2.4}$$

with parameters σ_S, σ_v, κ, θ_t, α and $\gamma > 0$. The volatility in expression (2.4) reflects the so-called Samuelson effect, which describes an empirical observation of the variations in futures prices increasing as the expiration date gets closer (see also Samuelson (1965)).[2] Figure 2a shows the time dependency for the implied volatilities in the HH natural gas market. These volatilities are grouped by the contracts' maturity month and then averaged. An inverse time-dependent pattern can be clearly observed in the data, providing evidence of the Samuelson effect in this market.

2.1.1 Seasonality specifications

In Hylleberg (1992), the seasonality is defined as "…the systematic, although not necessarily regular, intra-year movement caused by the changes of the weather, the calendar, and timing of decisions, directly or indirectly through the production and consumption decisions made by agents of the economy. These decisions are influenced by endowments, the expectations and preferences of the agents, and the production techniques available in the economy." Several models incorporate SSV in the trading date t such as RS02, GN05, ABP16, FMM16 and ST21. The first two are spot models which explicitly present seasonality in prices and variance; the last three are term-structure models which implicitly incorporate it in prices, explicitly in the variance. Other models such as FS19 explicitly present it in the variance in the delivery period rather than in the trade date, which is reasonable in electricity markets.

---

[2] This applies for a fixed maturity. Similarly, this effect can be seen in the futures variations which are, on a fixed date, higher for those contracts with longer maturities. When t approaches T, the term converges to 1 and the full volatility enters the dynamics. On the contrary, the volatility decreases when the time to maturity increases. This approach is typically captured with a term-structure alteration in the diffusion of the futures dynamics of the form followed by $\sigma_y(t, T)$ in expression (2.4).

As indicated in BPR13, implied volatilities in option prices reflect how market participants assess the future volatility pattern. In Fig. 2b we show the seasonality for the quoted volatilities in the HH natural gas market. These volatilities are grouped by the options' trade month and then averaged. A trigonometric function describes the seasonal pattern in implied volatilities with reasonable accuracy. Thus we present two seasonality functions for θ_t that can be used as parametric forms to model seasonal variations of futures prices's volatility. These functions are deterministic and work with the following parameters: $a^\theta > 0; b^\theta, c^\theta \neq 0$ and $t_0 \in [0, 1[$. The parameter a^θ determines the basic volatility level, b^θ and c^θ govern the magnitude of the seasonality pattern, and t_0 refers to the time of the year when the volatility reaches its maximum. The simple (S) and multiple or mixed (M) harmonic expressions are defined as follows

$$\theta_t^S \equiv a^\theta + b^\theta \cos\big(2\pi(t - t_0)\big), \tag{2.5}$$

$$\theta_t^M \equiv a^\theta + b^\theta \cos\big(2\pi(t - t_0)\big) + c^\theta \sin\big(2\pi(t - t_0)\big), \tag{2.6}$$

which are continuous functions, differentiable everywhere and spend the same amount of time low and high.

The form followed by the simple seasonality pattern S is inspired in the work of FS19 and ST21. Using the property of complementary angles, adapting the expression followed by θ_t^S in (2.5) is straightforward in terms of using the sinus instead of the cosinus of the angle.[3] With regards to the combined harmonic expression, the expression followed by θ_t^M in (2.6) is inspired in Rogel-Salazar and Sapsford (2014).

The specification followed by the variance dynamics can only guarantee the positiveness of the factor at all times if the Feller condition is met.[4] In our model, the sufficient condition to enforce the positivity of the variance is $2\kappa(a^\theta - b^\theta) > \sigma_v^2$ for the simple harmonic expression.[5]

In Fig. 3 we can observe futures prices and options volatilities for seven HH natural gas contracts labeled M2-M8, spanning from January 2011 to December 2020: Fig. 3a represents the time series for futures prices, Fig. 3b represents the ATM call option volatilities. In Fig. 4 we refer to the same futures contracts previously described: in Fig. 4a we plot the futures' returns, in Fig. 4b we represent the histogram of frequencies assigned to these returns, in Fig. 4c we display the correspondent QQ plot. From them we can observe the presence of fat tails in their distribution and conclude that returns are non-iid. Directly related to what we can observe in this figure, Table 2 provides complementary evidence of the non-Gaussian returns by rejecting the null hypothesis of normal price returns by means of the Jarque–Bera test, applicable to each contract individually and all contracts taken together.

In the natural gas market, where price returns are non-Gaussian, there are different possibilities to address an appropriate modeling strategy. Apart from the cyclical pattern driven by the supply side, we empirically observe the existence of shocks in prices, positive and negative. The ILE links large positive returns with increasing periods in the variance, but we also observe negative jumps. In this work, we decide to focus only on the seasonality, capturing it in an effective manner. Since the presence of the ILE justifies the presence of positive jumps, indirectly our model accounts for them. We do not introduce negative jumps in this research but their inclusion can be a natural future extension of this work.

---

[3] By adding $3/12$ to the value of t_0.

[4] In Heston (1993), the parameters obey that $2\kappa\theta > \sigma_v^2$, which is when the values of v_t are strictly positive. We also consider this restriction is met in all other multi-factor models analysed in this work.

[5] For the multiple harmonic expression, the condition depends on the minimum value achieved by a combination of the sinus and cosinus functions, reaching their minimum in different points.

(a) Futures Prices

(b) Option Volatilities
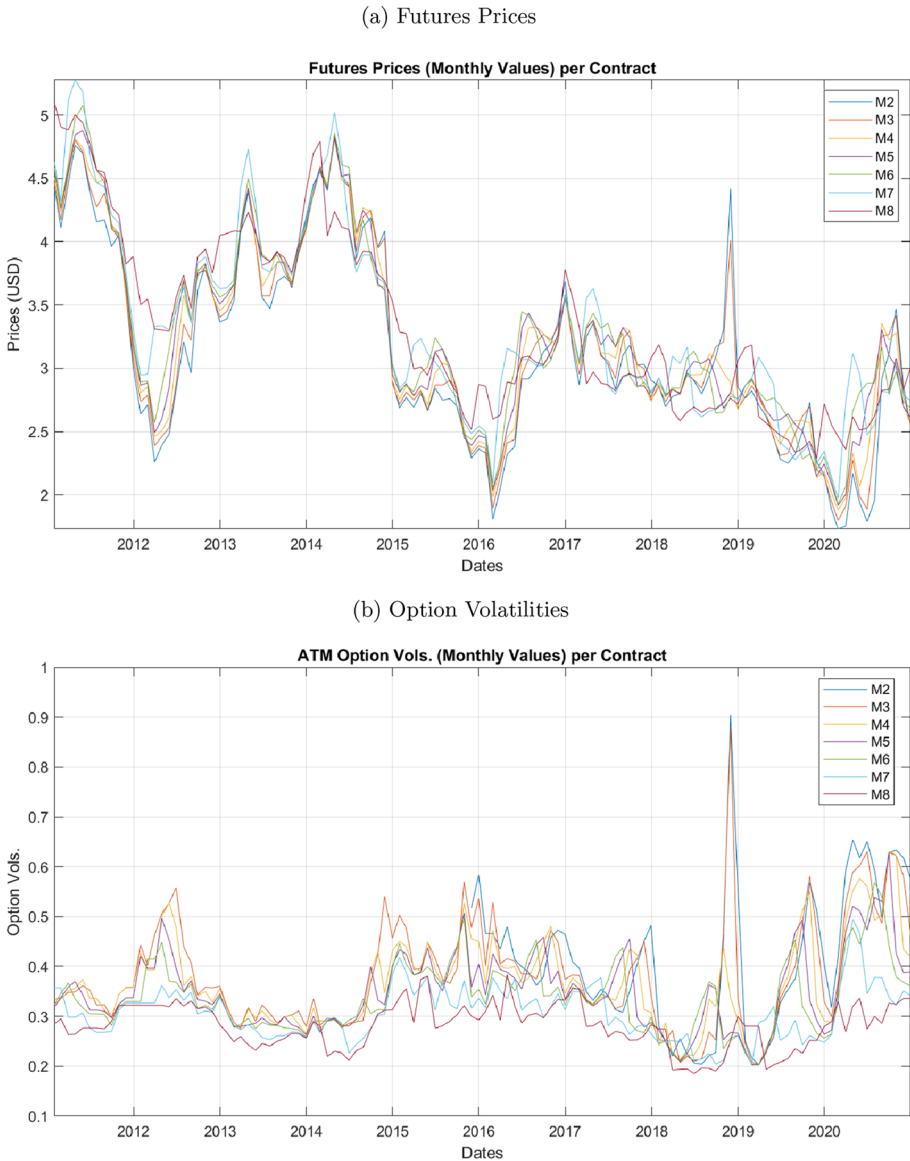
Fig. 3 Futures prices and ATM options volatilitites—monthly data. *Notes*: **a** presents the prices of the futures contracts labeled M2–M8. **b** presents the volatilities of quoted ATM call options on the futures labeled M2-M8. All values correspond to monthly observations

2.1.2 Futures dynamics

In this section we present a novel formulation for the futures' dynamics, which consists of an extension of TS09-SV1 that includes SSV. Let $F(t, T)$ denote the time-t price of a futures contract that matures at time T. By definition we have that

(a) Futures Returns

(b) Histogram of Returns

(c) QQ Plot
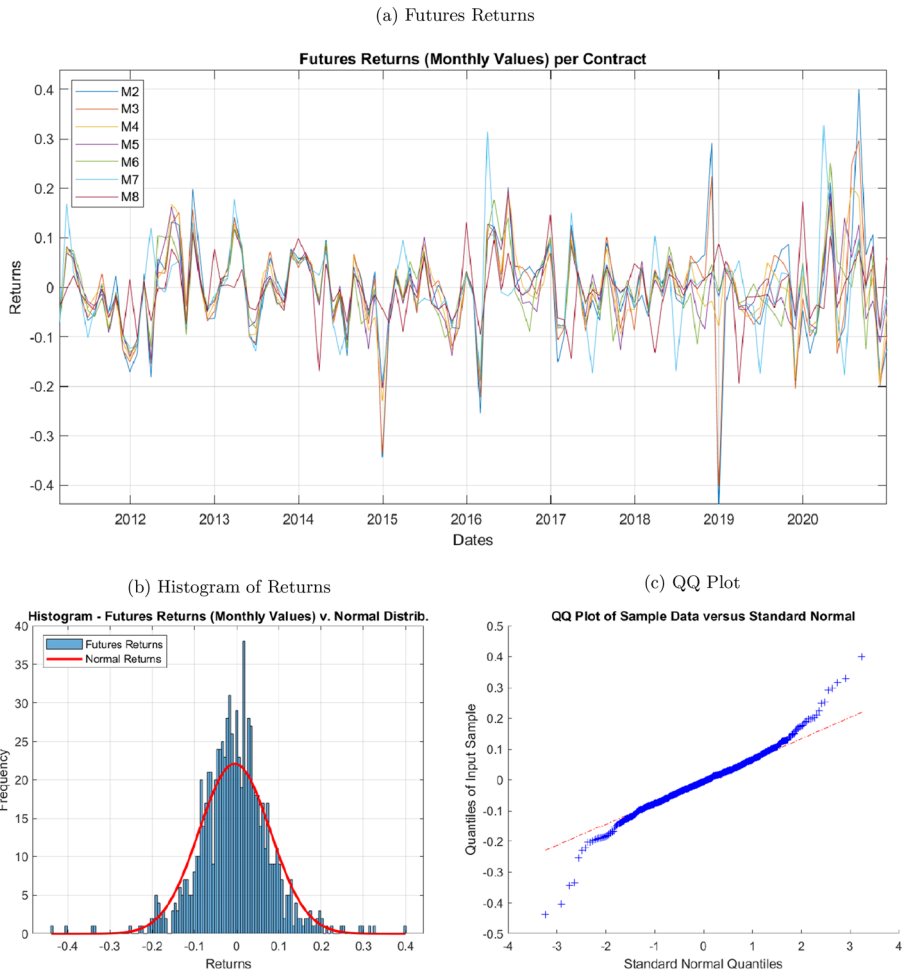
Fig. 4 Futures returns—monthly data. *Notes*: **a** presents the returns of the futures contracts labeled M2-M8. In **b** we can see in blue the correspondent histogram to the returns in **a**, the curve in red represents the equivalent PDF of a normal distribution with the same mean and standard deviation. In **c** we can see in blue the correspondent QQ plot to the returns, the red line represents the normal distribution and the blue points represent our sample returns. All values correspond to monthly observations

$$F(t, T) \equiv S_t \exp\left\{ \int_t^T y(t, u)du \right\} = S_t e^{Y(t,T)} \tag{2.7}$$

with dynamics of S_t and $y(t, T)$ as in Eqs. (2.1) and (2.2). In absence of arbitrage opportunities, the process followed by $F(t, T)$ must be a martingale under the risk-neutral measure $\mathbb{Q}$ (see Duffie (2001)). We define $f(t, T) \equiv \ln F(t, T)$, with $F(0, T) > 0$, $f(0, T) \neq 0$. From applying Itô's Lemma to the futures price in Eq. (2.7) and imposing the martingale condition (that is, setting the drift to zero), it follows that the dynamics of $F(t, T)$ and $f(t, T)$ are given by

$$\frac{dF(t, T)}{F(t, T)} = \sqrt{v_t}\left(\sigma_S dW_t^S + \sigma_Y(t, T)dW_t^y \right), \tag{2.8}$$

$$df(t, T) = \sqrt{v_t}\Big(\sigma_S dW_t^S + \sigma_Y(t, T)dW_t^y\Big) - \frac{v_t}{2}\Big(\sigma_S^2 + \sigma_Y^2(t, T) + 2\rho_{Sy}\sigma_S\sigma_Y(t, T)\Big)dt, \tag{2.9}$$

with the accumulated volatility of $y(t, T)$ being

$$\sigma_Y(t, T) \equiv \int_t^T \sigma_y(t, u)du = \frac{\alpha}{\gamma}\left(1 - e^{-\gamma(T-t)}\right), \tag{2.10}$$

and the drift term in Eq. (2.2) given by

$$\mu_y(t, T) = -\Big(\sigma_S\rho_{Sy} + \sigma_Y(t, T)\Big)\sigma_y(t, T)v_t. \tag{2.11}$$

The proof can be found in Trolle & Schwartz (2009, Appendix A).

We define the futures dynamics based on firstly describing the dynamics of the spot price and the forward cost of carry curve, to then modify the diffusion term in the futures dynamics accordingly by introducing the accumulated volatility expression instead; that is, $\sigma_Y(t, T)$ in expression (2.10). Our model for futures prices is then defined by Eqs. (2.8) and (2.3) Rewriting the dynamics in Eqs. (2.8) and (2.9) in their integral form time 0 up to time $t \leq T$ lets us see the evolution of futures prices and log-prices

$$F(t, T) = F(0, T)\exp\left\{\int_0^t \sqrt{v_u}\Big(\sigma_S dW_u^S + \sigma_Y(u, T)dW_u^y\Big) - \frac{1}{2}\int_0^t v_u\Big(\sigma_S dW_u^S + \sigma_Y(u, T)dW_u^y\Big)^2\right\}, \tag{2.12}$$

$$f(t, T) = f(0, T) + \int_0^t \sqrt{v_u}\Big(\sigma_S dW_u^S + \sigma_Y(u, T)dW_u^y\Big) - \frac{1}{2}\int_0^t v_u\Big(\sigma_S dW_u^S + \sigma_Y(u, T)dW_u^y\Big)^2, \tag{2.13}$$

with

$$\Big(\sigma_S dW_u^S + \sigma_Y(u, T)dW_u^y\Big)^2 = \Big(\sigma_S^2 + \sigma_Y^2(u, T) + \sigma_S\sigma_Y(u, T)\rho_{Sy}\Big)du.$$

Following Crosby & Frau (2022, Sec. 3), we refer to this set-up as the original characterisation of the parameters, where the expressions are defined in terms of S_t and $y(t, T)$ $(\sigma_S, \sigma_Y(t, T), \rho_{Sy}, \rho_{Sv}, \rho_{vy})$.

Alternative Characterisation of the Parameters
Evidence supports considering that the volatility of the futures $\sigma_f(t, T)$ follows a time-dampening form such as

$$\sigma_f(t, T) = \alpha_0 + \alpha e^{-\gamma(T-t)}. \tag{2.14}$$

Therefore, the expression which describes the volatility of the futures dynamics is

$$\sigma_F(t, T) \equiv \int_t^T \sigma_f(t, u)du = \alpha_0(T - t) + \frac{\alpha}{\gamma}\left(1 - e^{-\gamma(T-t)}\right). \tag{2.15}$$

This leads to more compact expressions defining the dynamics of the futures prices and log-prices

$$\frac{dF(t, T)}{F(t, T)} = \sqrt{v_t}\sigma_F(t, T)dW_t^F, \tag{2.16}$$

$$df(t, T) = \sqrt{v_t}\sigma_F(t, T)dW_t^F - \frac{1}{2}v_t\sigma_F^2(t, T)dt, \tag{2.17}$$

Table 2 Futures returns and Jarque–Bera test

Contract	Min. (%)	Max. (%)	Mean (%)	Std. Dev. (%)	Skew.	Kurt.	JB Stat.	p-value	Test
(a) Monthly observations									
M2	−43.82	40.02	−0.35	10.61	−0.2939	6.4480	5.929	0.0442	R
M3	−40.29	29.69	−0.34	9.77	−0.4977	5.7563	6.329	0.0396	R
M4	−22.97	20.21	−0.35	7.98	0.0011	3.3583	6.915	0.0331	R
M5	−20.31	19.83	−0.40	7.35	0.0527	3.1785	7.865	0.0258	R
M6	−18.99	25.15	−0.45	7.29	0.1753	3.4847	9.167	0.0190	R
M7	−18.90	32.80	−0.48	8.19	0.7649	5.9847	10.527	0.0142	R
M8	−19.50	17.25	−0.37	5.97	0.0752	4.3030	11.064	0.0127	R
ALL	−43.82	40.02	−0.39	8.27	−0.0700	6.0021	1567.737	0.0010	R
(b) Daily observations									
M2	−20.21	17.13	−0.02	2.43	0.1865	9.0481	119.964	0.0010	R
M3	−37.70	26.79	−0.02	2.34	−0.8969	38.3860	128.552	0.0010	R
M4	−10.11	22.96	−0.02	1.97	0.6833	11.7360	143.408	0.0010	R
M5	−13.87	14.89	−0.02	1.85	0.0712	8.9002	175.663	0.0010	R
M6	−11.32	13.26	−0.03	1.74	0.1228	8.6686	213.328	0.0010	R
M7	−12.80	14.00	−0.03	1.65	−0.1090	9.0187	228.004	0.0010	R
M8	−14.84	9.21	−0.02	1.85	−0.7251	10.2528	227.048	0.0010	R
ALL	−37.70	26.79	−0.02	1.96	−0.1119	18.9926	33600.777	0.0010	R

JB accounts for the Jarque–Bera normality test. The null hypothesis refers to the normal distribution of futures returns. The critical value associated to a significance level of 0.05 is 5.991. When the value of Test is R (CR), we reject (cannot reject) the null hypothesis at 95%

with W_t^F a Brownian motion defined for all $0 \leq t \leq T$. Rewriting the dynamics in (2.16)-(2.17) in their integral form from time 0 up to time $t \leq T$ lets us see the evolution of futures prices and log-prices

$$F(t, T) = F(0, T) \exp \left\{ \int_0^t \sqrt{v_u} \sigma_F(u, T) dW_u^F - \frac{1}{2} \int_0^t v_u \sigma_F^2(u, T) du \right\}, \qquad (2.18)$$

$$f(t, T) = f(0, T) + \int_0^t \sqrt{v_u} \sigma_F(u, T) dW_u^F - \frac{1}{2} \int_0^t v_u \sigma_F^2(u, T) du. \qquad (2.19)$$

Following Crosby & Frau (2022, Sec. 3), we refer to this set-up as the alternative characterisation of the parameters, where the expressions are defined in terms of $F(t, T)$. TS09-SV1 needs only 7 parameters instead of the original 9, whereas our model needs up to 8–9 instead of the original 10–11, depending on the expression chosen for θ_t. Therefore, our model is capable of replicating values generated with the original set-up using two parameters less, which makes calibration much quicker as can be observed in Table 8.

2.2 Deriving the characteristic function

Options on natural gas expire (T_{Opt}) one business day before the expiration date of the underlying futures contract T, that is, $T_{Opt} = T - 1/252$. The Fourier transform for the time-t standard European option price can be expressed in terms of the characteristic function (CF hereafter) $\psi(iu; t, T_{Opt}, T)$, so it can be obtained by applying the Fourier inversion theorem.

To price options on futures we introduce the transform

$$\psi(iu; t, T_{Opt}, T) \equiv E_t^{\mathbb{Q}}[e^{iuf(T_{Opt}, T)}], \tag{2.20}$$

with futures log-price dynamics as in Eq. (2.9) for the original set-up or (2.17) for the alternative one. We define $\tau \equiv T_{Opt} - t$. The transform (2.20) has an exponential affine solution as demonstrated in the following proposition:

Proposition 1 *The Fourier transform in Eq. (2.20) is given by*

$$\psi(iu; t, T_{Opt}, T) = e^{A(\tau) + B(\tau)v_t + iuf(t,T)}. \tag{2.21}$$

$A(\tau)$ *and* $B(\tau)$ *solve the following system of ODEs*

$$\frac{\partial A(\tau)}{\partial \tau} = B(\tau)\kappa\theta_t, \tag{2.22}$$

$$\frac{\partial B(\tau)}{\partial \tau} = b_0 + b_1 B(\tau) + b_2 B^2(\tau), \tag{2.23}$$

subject to the initial conditions $A(0) = B(0) = 0$, θ_t *as in (2.5) or (2.6). The expressions followed by the terms* b_0, b_1 *and* b_2 *conditional to the original set-up (left column) and the alternative set-up (right column) are*

$$b_0 = -\frac{1}{2}(u^2 + iu)\big(\sigma_S^2 + \sigma_Y^2(t, T) + 2\rho_{Sy}\sigma_S\sigma_Y(t, T)\big), \quad b_0 = -\frac{1}{2}(u^2 + iu)\sigma_F^2(t, T),$$

$$b_1 = -\kappa + iu\sigma_v\big(\rho_{Sv}\sigma_S + \rho_{yv}\sigma_Y(t, T)\big), \qquad\qquad b_1 = -\kappa + iu\sigma_v\rho_{Fv}\sigma_F(t, T),$$

$$b_2 = \frac{\sigma_v^2}{2}, \qquad\qquad\qquad\qquad\qquad\qquad\qquad\qquad b_2 = \frac{\sigma_v^2}{2}. \tag{2.24}$$

Proof See Appendix A.1 for proof.   □

The analytic expression followed by $B(\tau)$ in Eq. (2.21) is not affected by θ_t and reads

$$B(\tau) = \frac{2\gamma}{\sigma_v^2}\left(\beta + \mu z + z\frac{g'(z)}{g(z)}\right), \tag{2.25}$$

and the expressions followed by $\beta, \mu, z, g(z)$ and $g'(z)$ can be found in Appendix B.1.

The following two propositions provide the analytic expressions followed by $A(\tau)$ in Eq. (2.21).

Proposition 2 *When* θ_t *follows a single sinusoidal form as in expression (2.5), ODE (2.22) has a quasi-analytical solution which is given by*

$$A(\tau) = m\big(A_1(\tau) + A_2(\tau) + A_3(\tau) + A_4(\tau) + k_3\big), \tag{2.26}$$

with

$$A_1(\tau) = a^\theta\left(\beta\tau - \frac{\mu z + \ln g(z)}{\gamma}\right),$$

$$A_2(\tau) = -b^\theta\frac{\beta y_\tau^s}{2\pi},$$

$$A_3(\tau) = b^\theta\mu z\frac{y_\tau^c - 2\pi\gamma y_\tau^s}{4\pi^2 + \gamma^2}, \tag{2.27}$$

$$A_4(\tau) = b^\theta\frac{\tau}{\omega}\left(y_0^c g'(\omega^{-1}) - \frac{\tau}{2}\big(g'(\omega^{-1})\big(y_0^c\zeta_1 - 2\pi y_0^c\big) + y_0^c\zeta_2\big)\right),$$

with a, b, β, μ, z, $g(z)$ and $g(z)$ as defined in Appendix B.1, with

$$
\begin{aligned}
m &= \frac{2\kappa\gamma}{\sigma_v^2}, \\
y_\tau^c &= \cos\left(2\pi\left(T_0 - \tau - t_0\right)\right), \quad y_0^c = \cos\left(2\pi\left(T_0 - t_0\right)\right), \\
y_\tau^s &= \sin\left(2\pi\left(T_0 - \tau - t_0\right)\right), \quad y_0^s = \sin\left(2\pi\left(T_0 - t_0\right)\right), \\
\zeta_1 &= \gamma(1 + k_1 n_1 + k_2 n_2), \qquad \zeta_2 = \gamma(k_1 n_3 + k_2 n_4),
\end{aligned}
\tag{2.28}
$$

and

$$
\begin{aligned}
n_1 &= (a-b)\big(M(a-1,b,\omega^{-1}) - M(a,b,\omega^{-1})\big) + M(a,b,\omega^{-1})\omega^{-1}, \\
n_2 &= a\big(U(a,b,\omega^{-1}) + (b-a-1)\,U(a+1,b,\omega^{-1})\big), \\
n_3 &= \frac{a}{b}\Big((a-b)\big(M(a+1,b+1,\omega^{-1}) - M(a,b+1,\omega^{-1})\big) + M(a+1,b+1,\omega^{-1})\omega^{-1}\Big), \\
n_4 &= a\big(U(a,b,\omega^{-1}) + \left(b-\omega^{-1}\right)U(a+1,b+1,\omega^{-1})\big).
\end{aligned}
\tag{2.29}
$$

M and U are Kummer's and Tricomi's hypergeometric functions, as defined in Appendix B.1.

In particular, if the initial condition is $A(0) = 0$, we have that

$$
\begin{aligned}
k_3 &= x_0 + x_0^s y_0^s + x_0^c y_0^c, \\
x_0 &= a^\theta \frac{\mu}{\omega}, \\
x_0^s &= b^\theta\left(\frac{\beta}{2\pi} - \frac{2\pi\mu}{\omega(4\pi^2 + \gamma^2)}\right), \\
x_0^c &= -b^\theta \frac{\mu\gamma}{\omega(4\pi^2 + \gamma^2)}.
\end{aligned}
\tag{2.30}
$$

Proof See Appendix A.2 proof.   □

Proposition 3 *When θ_t follows a mixed sinusoidal form as in expression (2.6), ODE (2.22) has a quasi-analytical solution which is given by*

$$
A(\tau) = m\big(A_1(\tau) + A_2(\tau) + A_3(\tau) + A_4(\tau) + A_5(\tau) + A_6(\tau) + A_7(\tau) + k_3\big), \tag{2.31}
$$

with $A_1(\tau)$, $A_2(\tau)$, $A_3(\tau)$ and $A_4(\tau)$ as in Proposition 2, with

$$
\begin{aligned}
A_5(\tau) &= c^\theta \beta \frac{y_\tau^c}{2\pi}, \\
A_6(\tau) &= c^\theta \mu z \frac{2\pi y_\tau^s - \gamma y_\tau^c}{4\pi^2 + \gamma^2}, \\
A_7(\tau) &= c^\theta \frac{\tau}{\omega}\left(y_0^s g'(\omega^{-1}) - \frac{\tau}{2}\big(g'(\omega^{-1})\left(y_0^s \zeta_1 + 2\pi y_0^c\right) + y_0^s \zeta_2\big)\right),
\end{aligned}
\tag{2.32}
$$

with β, μ, z, $g(z)$ and $g(z)$ as defined in Appendix B.1; m, y_τ^c, y_0^c, y_τ^s, y_0^s, ζ_1 and ζ_2 as in expression (2.28).

In particular, if the initial condition is $A(0) = 0$, we have that

$$
\begin{aligned}
k_3 &= x_0 + x_0^s \, y_0^s + x_0^c \, y_0^c, \\
x_0 &= a^\theta \frac{\mu}{\omega}, \\
x_0^s &= b^\theta \left(\frac{\beta}{2\pi} + \frac{2\pi\mu}{\omega(4\pi^2 + \gamma^2)} \right) - c^\theta \frac{\mu\gamma}{\omega(4\pi^2 + \gamma^2)}, \\
x_0^c &= -b^\theta \frac{\mu\gamma}{\omega(4\pi^2 + \gamma^2)} + c^\theta \left(\frac{\beta}{2\pi} + \frac{2\pi\mu}{\omega(4\pi^2 + \gamma^2)} \right).
\end{aligned}
\tag{2.33}
$$

Proof See Appendix A.3 for proof. $\qquad\square$

In Proposition 2, if $b^\theta = 0$ we then have that $\theta_t = a^\theta$, $A_2(\tau) = A_3(\tau) = A_4(\tau) = 0$, and $A(\tau) = A_1(\tau)$. In Proposition 3, if $b^\theta = c^\theta = 0$ we have that $\theta_t = a^\theta$, $A_2(\tau) = A_3(\tau) = A_4(\tau) = A_5(\tau) = A_6(\tau) = A_7(\tau) = 0$, and therefore $A(\tau) = A_1(\tau)$. Under either situation, our model is equivalent to TS09-SV1 and $A(\tau)$ reads

$$
\begin{aligned}
A(\tau) &= m(A_1(\tau) + k_3^{TS}), \\
k_3^{TS} &= x_0 = a^\theta \frac{\mu}{\omega}.
\end{aligned}
\tag{2.34}
$$

Independently of the harmonic expression chosen and based on evidence, we assume that in the long-run mean-reverting parameter θ_t there is only one peak per year.

2.2.1 Extant models

The naturally nested model respective to ours is TS09-SV1. Additionally, we also consider other extant models such as Mer76, Hes93 and Bat96. We compare the performance of our model to jump-diffusion models to avoid misinterpreting cycles in prices as jumps. We also include ST18 and ST21 in the list of extant models, the latter presenting SSV.[6]

Modeling the futures dynamics using jumps and stochastic volatility results in the futures prices having non-Gaussian returns—a stylised fact in the energy markets. In Table 2 we present the values for the four first moments of the distribution, and we perform the Jarque–Bera normality test on monthly data. We reject the null hypothesis of normality in returns for each of the labeled contracts M2-M8, and all contracts taken together. This implies that some source of structure in the variance such as stochastic volatility is required, providing skewness and/or kurtosis to the distribution of returns. Many earlier models include stochastic volatility in their specification.

We consider one-, two- and three-factor extant models, a mix of spot-based and term-structure models. To compare them from a commodity perspective, we transform the original spot-based specification in Mer76, Hes93 and Bat96 to their corresponding futures prices dynamics.[7] Hereafter we will refer to their futures-equivalent specification, but naming them in their original form. In this work we consider a panel of six extant models plus ours; in Sect. 4 we compare their pricing performances.

---

[6] In this work, we consider the one-dimensional specification of both models (that is, $i = 1$). Following this restriction and only in the case that we impose the constant term $\alpha = 0$ to the original specifications of TS09-SV1 and our model SYSSV, we have that TS09-SV1 and SYSSV are quite similar to ST18 and ST21, respectively; they only differ in the expression followed by the future's volatility term—for the first, it is an accumulated form of that of the latter.

[7] Option prices for commodities's futures are quoted in the markets using Black (1976).

Table 3 Models dynamics

Model	Dynamics	Volatility
BS73	$\frac{dS_t}{S_t} = ydt + \sigma_S dW_t^S$	σ_S constant
	$\frac{dF(t,T)}{F(t,T)} = \sigma_F dW_t^F$	σ_S constant
Mer76	$\frac{dS_t}{S_t} = \left(y - \lambda E_t^{\mathbb{Q}}\left[e^{J_S} - 1\right]\right)dt + \sigma_S dW_t^S + \left(e^{J_S} - 1\right)dN_t$	σ_S constant
	$\frac{dF(t,T)}{F(t,T)} = -\lambda E_t^{\mathbb{Q}}\left[e^{J_F} - 1\right]dt + \sigma_F dW_t^F + \left(e^{J_F} - 1\right)dN_t$	σ_F constant
Hes93	$\frac{dS_t}{S_t} = ydt + \sqrt{v_t}dW_t^S$	$\sigma_S = 1$
	$dv_t = \kappa\left(\theta - v_t\right)dt + \sigma_v\sqrt{v_t}dW_t^v$	σ_v constant
	$\frac{dF(t,T)}{F(t,T)} = \sigma_F\sqrt{v_t}dW_t^F$	σ_F constant
Bat96	$\frac{dS_t}{S_t} = \left(y - \lambda E_t^{\mathbb{Q}}\left[e^{J_S} - 1\right]\right)dt + \sqrt{v_t}dW_t^S + \left(e^{J_S} - 1\right)dN_t$	$\sigma_S = 1$
	$dv_t = \kappa\left(\theta - v_t\right)dt + \sigma_v\sqrt{v_t}dW_t^v$	σ_v constant
	$\frac{dF(t,T)}{F(t,T)} = -\lambda E_t^{\mathbb{Q}}\left[e^{J_F} - 1\right]dt + \sqrt{v_t}dW_t^F + \left(e^{J_F} - 1\right)dN_t$	σ_F constant
TS09-SV1	$\frac{dS_t}{S_t} = y_t dt + \sigma_S\sqrt{v_t}dW_t^S$	σ_S constant
	$dy(t,T) = \mu_y(t,T)dt + \sigma_y(t,T)\sqrt{v_t}dW_t^y$	$\sigma_y(t,T) = \alpha e^{-\gamma(T-t)}$
	$dv_t = \kappa\left(\theta - v_t\right)dt + \sigma_v\sqrt{v_t}dW_t^v$	σ_v constant
	$\frac{dF(t,T)}{F(t,T)} = \sqrt{v_t}\left(\sigma_S dW_t^S + \sigma_Y(t,T)dW_t^y\right)$	$\sigma_Y(t,T) = \int_t^T \sigma_y(t,u)du$
TS09-SV1*	$\frac{dF(t,T)}{F(t,T)} = \sigma_F(t,T)\sqrt{v_t}dW_t^F$	$\sigma_f(t,T) = \alpha_0 + \alpha e^{-\gamma(T-t)}, \alpha = 1$
		$\sigma_F(t,T) = \int_t^T \sigma_f(t,u)du$
ST18	$\frac{dF(t,T)}{F(t,T)} = \sum_{i=1}^n \sigma_{F_i}(t,T)\sqrt{v_{i,t}}dW_t^{F_i}$	$\sigma_{F_i}(t,T) = e^{-\gamma_i(T-t)}, \alpha_i = 1$
	$dv_{i,t} = \kappa_i\left(\theta_i - v_{i,t}\right)dt + \sigma_{v_i}\sqrt{v_{i,t}}dW_t^{v_i}$	σ_{v_i} constant
ST21	$\frac{dF(t,T)}{F(t,T)} = \sum_{i=1}^n \sigma_{F_i}(t,T)\sqrt{v_{i,t}}dW_t^{F_i}$	$\sigma_{F_i}(t,T) = e^{-\gamma_i(T-t)}, \alpha_i = 1$
	$dv_{i,t} = \kappa_i\left(\theta_t - v_{i,t}\right)dt + \sigma_{v_i}\sqrt{v_{i,t}}dW_t^{v_i}$	σ_{v_i} constant
	$\theta_t = a^\theta + b^\theta\cos(2\pi(t + t_0))$	
SYSSV	$\frac{dS_t}{S_t} = y_t dt + \sigma_S\sqrt{v_t}dW_t^S$	σ_S constant
	$dy(t,T) = \mu_y(t,T)dt + \sigma_y(t,T)\sqrt{v_t}dW_t^y$	$\sigma_y(t,T) = \alpha e^{-\gamma(T-t)}, \alpha = 1$
	$dv_t = \kappa\left(\theta_t - v_t\right)dt + \sigma_v\sqrt{v_t}dW_t^v$	σ_v constant
	$\theta_t^S = a^\theta + b^\theta\cos(2\pi(t + t_0))$	
	$\theta_t^M = a^\theta + b^\theta\cos(2\pi(t + t_0)) + c^\theta\sin(2\pi(t + t_0))$	
	$\frac{dF(t,T)}{F(t,T)} = \sqrt{v_t}\left(\sigma_S dW_t^S + \sigma_Y(t,T)dW_t^y\right)$	$\sigma_Y(t,T) = \int_t^T \sigma_y(t,u)du$
SYSSV*	$\frac{dF(t,T)}{F(t,T)} = \sigma_F(t,T)\sqrt{v_t}dW_t^F$	$\sigma_f(t,T) = \alpha_0 + \alpha e^{-\gamma(T-t)}, \alpha = 1$
		$\sigma_F(t,T) = \int_t^T \sigma_f(t,u)du$

This table presents the model dynamics and their correspondent volatility expressions for the models described in Sect. 2.2.1 and our model SYSSV. S_t denotes the time-t spot price of the commodity; $y(t,T)$ denotes the time-t instantaneous forward cost of carry maturing at time T, with $y(t,t) = y_t$ the time-t instantaneous spot cost of carry; v_t denotes the instantaneous variance. For the first four models, the last equation refers to their corresponding futures' price dynamics. Those models presenting an alternative set-up of the parameters (i.e., TS09-SV1 and SYSSV) appear with the symbol $\star$
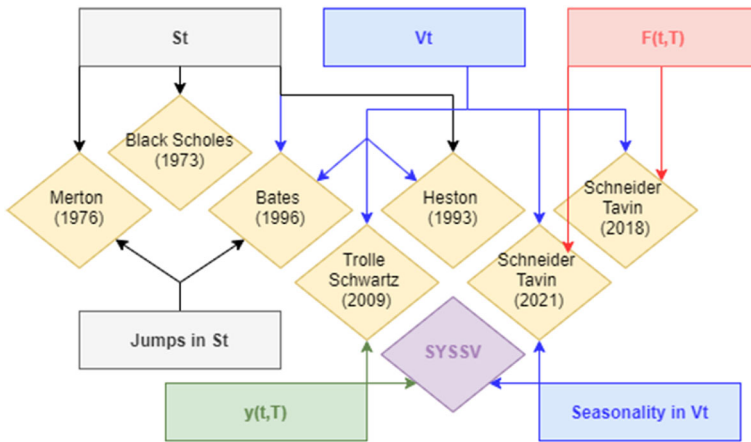
Fig. 5 Diagram of extant models. *Notes:* In this figure we represent in a visual manner the factors affecting each of the considered models in this work, the existence of the type of seasonal effect and/or jumps. This figure complements the information in Sect. 2.2.1 and Table 3

For each model, next we describe the components of the Fourier transform described in Eq. (2.21). BS73 models the spot prices requiring only the independent term $A(\tau)$; Mer76 extends BS73 incorporating iid jumps in the spot price, the jump-related terms are included in $A(\tau)$; Hes93 extends BS73 with stochastic variance, it uses $A(\tau)$ and the stochastic variance-related term $B(\tau)$; Bat96 extends Hes93 with iid jumps in the spot price, it uses $A(\tau)$ and $B(\tau)$; TS09-SV1, ST18, ST21 and our model are term-structure models with stochastic prices and variances, which require both terms $A(\tau)$ and $B(\tau)$. For instance, ST21 and our model incorporate seasonality in the variance, whereas TS09-SV1 and ST18 do not. Both TS09-SV1 and our model describe the dynamics of the spot price and the cost of carry before obtaining the futures' dynamics.

In Table 3 we present the dynamics followed by the models in the above list as well as ours. This table is complemented by Fig. 5, which visually represents the links between the different models in terms of factors, seasonality and jumps. The expressions followed by the dynamics of $A(\tau)$ and $B(\tau)$ in Eq. (2.21) and their solutions can be found in Tables 4 and 5, respectively.

Key advantages of the most recent models encompassing ours include improved approximation to the real price behaviour and better description of the implied volatility surface. In our case, adding up to three seasonality-related parameters provides more flexibility to replicate the volatility surface quoted in the market, allowing for a wider range of possible shapes (e.g., the Samuelson effect and the seasonal temperatures affecting the natural gas demand). The implementation is not straightforward; it does not require the addition of new terms to the CF in TS09-SV1, but the variance-related term $B(\tau)$ must be modified due to the seasonal component introduced.

2.3 Pricing of standard European options

In this section we price standard European options on futures contracts using the CF previously computed. Let $\mathcal{C}(t, T_{Opt}, T, K)$ and $\mathcal{P}(t, T_{Opt}, T, K)$ denote the time-t prices of a standard European call (hereafter, call) and a standard European put (hereafter, put) option expiring at time T_{Opt} with strike K on a futures contract expiring at time T, with

Table 4 Fourier transforms—ODEs and parameters

(a) ODEs

Model	$\partial A(\tau)/\partial\tau$	$\partial B(\tau)/\partial\tau$
BS73	b_0	—
Mer76	$b_0 + (n_J - ium_J)$	—
Hes93	$B(\tau)\kappa\theta$	$b_0 + b_1 B(\tau) + b_2 B^2(\tau)$
Bat96	$B(\tau)\kappa\theta + (n_J - ium_J)$	$b_0 + b_1 B(\tau) + b_2 B^2(\tau)$
TS09-SV1	$B(\tau)\kappa\theta$	$b_0 + b_1 B(\tau) + b_2 B^2(\tau)$
ST18	$B(\tau)\kappa\theta$	$b_0 + b_1 B(\tau) + b_2 B^2(\tau)$
ST21	$B(\tau)\kappa\theta_t$	$b_0 + b_1 B(\tau) + b_2 B^2(\tau)$
SYSSV	$B(\tau)\kappa\theta_t$	$b_0 + b_1 B(\tau) + b_2 B^2(\tau)$

(b) Parameters

Model	b_0	b_1	b_2
BS73	$-\frac{\sigma_S^2}{2}$	—	—
Mer76	$-\frac{\sigma_S^2}{2}$	—	—
Hes93	$-\frac{1}{2}(u^2 + iu)$	$-\kappa + iu\sigma_v\rho_{Sv}$	$\frac{\sigma_v^2}{2}$
Bat96	$-\frac{1}{2}(u^2 + iu)$	$-\kappa + iu\sigma_v\rho_{Sv}$	$\frac{\sigma_v^2}{2}$
TS09-SV1$^{\checkmark}$	$-\frac{1}{2}(u^2 + iu)(\sigma_S^2 + \sigma_Y^2(t,T) + 2\rho_{Sy}\sigma_S\sigma_Y(t,T))$	$-\kappa + iu\sigma_v(\rho_{Sv}\sigma_S + \rho_{yv}\sigma_Y(t,T))$	$\frac{\sigma_v^2}{2}$
TS09-SV1*	$-\frac{1}{2}(u^2 + iu)\sigma_F^2(t,T)$	$-\kappa + iu\sigma_v\rho_{Fv}\sigma_F(t,T)$	$\frac{\sigma_v^2}{2}$
ST18	$-\frac{1}{2}(u^2 + iu)\sigma_F^2(t,T)$	$-\kappa + iu\sigma_v\rho_{Fv}\sigma_F(t,T)$	$\frac{\sigma_v^2}{2}$
ST21	$-\frac{1}{2}(u^2 + iu)\sigma_F^2(t,T)$	$-\kappa + iu\sigma_v\rho_{Fv}\sigma_F(t,T)$	$\frac{\sigma_v^2}{2}$
SYSSV$^{\checkmark}$	$-\frac{1}{2}(u^2 + iu)(\sigma_S^2 + \sigma_Y^2(t,T) + 2\rho_{Sy}\sigma_S\sigma_Y(t,T))$	$-\kappa + iu\sigma_v(\rho_{Sv}\sigma_S + \rho_{yv}\sigma_Y(t,T))$	$\frac{\sigma_v^2}{2}$
SYSSV*	$-\frac{1}{2}(u^2 + iu)\sigma_F^2(t,T)$	$-\kappa + iu\sigma_v\rho_{Fv}\sigma_F(t,T)$	$\frac{\sigma_v^2}{2}$

This table presents the expressions followed by the ODEs for the models described in Sect. 2.2.1 and our model SYSSV. Observe that BS73, Mer76, Hes93 and Bat96 are expressed in terms of the futures prices. The expression followed by $\sigma_F(t, T)$ in each model can be found in Table 3. The expressions followed by the jump terms are

$$n_J = e^{iu\mu_J - \frac{1}{2}\sigma_J^2 u^2} - 1, \qquad m_J = e^{\mu_J + \frac{1}{2}\sigma_J^2} - 1, \qquad (2.35)$$

with μ_J and σ_J^2 corresponding to the mean and the variance of the jump in the price, respectively

$0 < t < T < T_{Opt}$. This option can be priced quasi-analytically within the framework we describe in this section. In our empirical work and from the different pricing approaches based on the CF, we follow the fast Fourier transform (FFT) methodology.[8]

2.3.1 The fast Fourier transform

Carr and Madan (1999) obtain a pricing formula for options which enables a computationally efficient FFT algorithm. Its popularity stems from its remarkable speed: while prior computation approaches require N^2 operations, the FFT requires only $N \ln(N)$ steps.

---

[8] See, e.g., Schmelzle (2010) for a classification of the different Fourier-based approaches.

Table 5 Fourier transforms—solutions to ODEs

Model	$A(\tau)$	$B(\tau)$
BS73	$b_0 \tau$	–
Mer76	$(b_0 + n_J - iu m_J)\tau$	–
Hes93	$\frac{\kappa\theta}{\sigma_v^2}\left((\kappa - iu\sigma_v\rho_{Fv} - d)\tau - 2\ln\frac{1-ge^{-d\tau}}{1-g}\right)$	$\frac{\kappa - iu\sigma_v\rho_{Fv} - d}{\sigma_v^2}\left(\frac{1-e^{-d\tau}}{1-ge^{-d\tau}}\right)$
Bat96	$\frac{\kappa\theta}{\sigma_v^2}\left((\kappa - iu\sigma_v\rho_{Fv} - d)\tau - 2\ln\frac{1-ge^{-d\tau}}{1-g}\right)+(n_J - iu m_J)\tau$	$\frac{\kappa - iu\sigma_v\rho_{Fv} - d}{\sigma_v^2}\left(\frac{1-e^{-d\tau}}{1-ge^{-d\tau}}\right)$
TS09-SV1	$\frac{2\kappa\theta}{\sigma_v^2}\left(\beta\gamma\tau - \mu z - \ln g(z)\right)+k_3$	$\frac{2\gamma}{\sigma_v^2}\left(\beta + \mu z + z\frac{g'(z)}{g(z)}\right)$
ST18	$\frac{2\kappa\theta}{\sigma_v^2}\left(\beta\gamma\tau - \mu z - \ln g(z)\right)+k_3$	$\frac{2\gamma}{\sigma_v^2}\left(\beta + \mu z + z\frac{g'(z)}{g(z)}\right)$
ST21	$A_1(\tau) + A_2(\tau) + A_3(\tau) + A_4(\tau) + k_3$	$\frac{2\gamma}{\sigma_v^2}\left(\beta + \mu z + z\frac{g'(z)}{g(z)}\right)$
SYSSV	$A_1(\tau) + A_2(\tau) + A_3(\tau) + A_4(\tau) + A_5(\tau) + A_6(\tau) + A_7(\tau) + k_3$	$\frac{2\gamma}{\sigma_v^2}\left(\beta + \mu z + z\frac{g'(z)}{g(z)}\right)$

$$A_1(\tau) = ma^\theta\left(\beta\tau - \frac{1}{\gamma}\left(\mu z + \ln g(z)\right)\right)$$

$$A_2(\tau) = -mb^\theta\frac{\beta}{2\pi}y_\tau^s$$

$$A_3(\tau) = mb^\theta\frac{\mu z}{4\pi^2+\gamma^2}\left(\gamma y_\tau^c - 2\pi y_\tau^s\right)$$

$$A_4(\tau) = mb^\theta\omega^{-1}\left(\tau\, y_0^c g'(\omega^{-1}) - \frac{\tau^2}{2}\left(g'(\omega^{-1})\left(y_0^c\zeta_1 - 2\pi y_0^s\right) + y_0^c\zeta_2\right)\right)$$

$$A_5(\tau) = mc^\theta\frac{\beta}{2\pi}y_\tau^c$$

$$A_6(\tau) = mc^\theta\frac{\mu z}{4\pi^2+\gamma^2}\left(2\pi y_\tau^s - \gamma y_\tau^c\right)$$

$$A_7(\tau) = mc^\theta\omega^{-1}\left(\tau\, y_0^s g'(\omega^{-1}) - \frac{\tau^2}{2}\left(g'(\omega^{-1})\left(y_0^s\zeta_1 + 2\pi y_0^c\right) + y_0^s\zeta_2\right)\right)$$

This table presents the correspondent solution to the ODEs presented in Table 4. Observe that BS73, Mer76, Hes93 and Bat96 are expressed in terms of the futures prices. As per our model SYSSV, these expressions correspond to (2.22)-(2.23). The terms b_0, b_1 and b_2 can be found in expressions (2.24). For TS09-SV1 and our model, z, $g(z)$, $g'(z)$, β and μ are in Appendix B.1. For ST18 and ST21, z, $g(z)$, $g'(z)$, β and μ are in Appendix B.2, m is as in expression (2.28). The expressions followed by k_3 in TS09-SV1 and SYSSV can be seen in Eqs. (2.34) and (2.30) or (2.33), correspondingly. The values for n_J, m_J and b_0, b_1 and b_2 can be found in Table 4. For BS73 and Mer96, observe that $\sigma_Y(t, T) = 0$ (equivalently, $\sigma_F = \sigma_S$). For Hes93 and Bat96, observe that $\sigma_S = 1$ and $\sigma_Y = 0$ (equivalently, $\sigma_F = \sigma_S = 1$); for these models, g and d read

$$g = \frac{\kappa - iu\sigma_v\rho_{Fv} + d}{\kappa - iu\sigma_v\rho_{Fv} - d}, \qquad d = \sqrt{(\kappa - iu\sigma_v\rho_{Fv})^2 + \sigma_v^2(u^2 + iu)} \qquad (2.36)$$

In the following proposition we present the expressions followed by call and a put option prices:

Proposition 4 *The time-t price of a call and a put option expiring at time T_{Opt} with strike K on a time-t futures contract expiring at time T is given by*

$$\mathcal{C}(t, T_{Opt}, T, K) = P(t, T_{Opt})\frac{e^{-\alpha\ln(K)}}{\pi}\int_0^\infty \Re\left[\frac{e^{-iu\ln(K)}\psi_t(u - i(1+\alpha); t, T_{Opt}, T)}{\alpha(\alpha + 1) - u^2 + iu(1 + 2\alpha)}\right]du,$$
$$(2.37)$$

$$\mathcal{P}(t, T_{Opt}, T, K) = P(t, T_{Opt})\frac{e^{-\alpha\ln(K)}}{\pi}\int_0^\infty \Re\left[\frac{e^{-iu\ln(K)}\psi_t(u - i(1-\alpha); t, T_{Opt}, T)}{\alpha(\alpha - 1) - u^2 + iu(1 - 2\alpha)}\right]du,$$
$$(2.38)$$

where $P(T_{Opt}, t)$ is the time-t price of a zero-coupon bond maturing at T_{Opt} and α is the control parameter.[9]

Proof The proof is in Carr and Madan (1999).   □

This approach presents two advantages: firstly, it permits the use of the computationally efficient FFT; secondly, it only requires the evaluation of one integral, as opposed to the two integrals required when using former perspectives as in Heston (1993) or Duffie et al. (2000).

3 Market data and parameters estimation

In this section we indicate how we perform the empirical analysis: firstly we describe the natural gas data set we work with to perform our empirical analysis, then we discuss the stylised facts inherent to this market, afterwards we describe the process we carry out to perform the calibration exercise to market data, and to conclude we interpret the values of the parameters' estimates accordingly to the empirical observations.

3.1 Market data

We consider HH natural gas futures and options traded on the New York Mercantile Exchange (NYMEX),[10] which we obtain from Refinitiv Eikon (formerly, Thomson-Reuters' Datastream). The data set consist of observations of closing prices (quoted in USD) for futures and market implied volatilities for the corresponding options. There are monthly contracts listed for the current year and the next 12 calendar years for both futures and options. For futures, trading months are the 72 consecutive months commencing with the next calendar month, and trading terminates three business days prior to the first calendar day of the delivery month. For options, trading months are the 12 consecutive months plus contracts extending up to 72 months and traded in a quarterly manner, and trading terminates at the close of business on the business day preceding the expiration of the underlying futures contract. There are 20 strike prices in increments of 0.05 USD above and below the ATM strike price in all months. The ATM strike price is nearest to previous day's close of the underlying futures contract.[11]

The 10-year period considered spans from January 3rd 2011 to December 31st 2020 and the market data set is at monthly and daily frequency. When the data is observed on a monthly basis, the observations correspond to the last business day of each month in the considered period. We are considering seven futures contracts labeled M2, M3, ..., M8[12] and their correspondent ATM and OTM quoted options, call and put, for 16 degrees of moneyness (ATM plus 15 degrees of moneyness, from the ATM level $\pm 0.05\,i$ USD, for $i = 1 : 15$ (that is, $\pm 0, 0.05, 0.1, \ldots, 0.75$)), making it 32 options per contract and 224 options per observation date. The number of monthly (daily) observations equals 120 (2,521), making it 840 (17,647) futures prices and 26,880 (564,480) options volatilities. From these volatilities,

---

[9] α has to be chosen to ensure that it makes the modified option price square-integrable and to obtain good numerical accuracy—a sufficient condition for the Fourier transform to exist. This parameter has to be wisely chosen as it might produce very oscillatory arguments of the integral if too big, or it might approach a point mass around 0 if too small.

[10] See other works focusing on hubs in Europe (e.g., Jotanovic and D'Ecclesia (2021)) and on hubs in both continents (e.g., Jana and Gosh (2022)).

[11] Contract specifications for futures and options on HH natural gas can be found at CMEhome.

[12] They are the second to the eighth available maturity contracts.

we consider 21,972 (526,142) as valid after a cleansing process, which results in 81.74% (93.21%).

3.2 Stylised facts

In this section we discuss and provide the empirical evidence in the natural gas market. We distinguish between stylised facts which correspond to prices and variances. When we refer to prices, we refer either to spots or futures; whereas when we refer to variances, we also mean volatilities. In the natural gas market, prices are mean-reverting, present seasonality and eventually jumps; and variances are also seasonal and present an ILE. Additionally, they exhibit USV and the Samuelson effect, the latter is described in Sect. 2.1. All these empirical observations are incorporated in our model.

Seasonality is a well-known empirical feature for many commodities, specially for those which depend on the natural cycle (weather or temperature) such as agriculturals and natural gas; this seasonality affects the whole term-structure of prices and of variance (the latter can be observed in Fig. 2b). Natural gas is driven by weather-related demand—prices rise up at the beginning of cold months (autumn) and start declining at the beginning of warm ones (spring); similarly occurs with volatilities. In a cross-sectional analysis, we can also find seasonality when grouping contracts by maturity month (January, February, etc.); for prices it can be seen in Fig. 1a; for volatilities in Fig. 1b. When grouping contracts by available maturity (M2, M3, etc.), we find evidence of the Samuelson effect since long-dated futures vary more than those close to maturity, as can be seen in Fig. 2a. In our model, we incorporate seasonality in the variance by means of a deterministic θ_t.

A particular market exhibits USV when volatility risk cannot be fully hedged solely using a portfolio of those assets. TS09 was the first stochastic volatility HJM-type for pricing commodity derivatives, which remarks that the advantage of working in this particular setting is that USV arises naturally. It is a phenomenon which they show is important in crude oil derivatives market. In Table 8, the innovation of the volatility factor has very low correlation with the innovation of the futures prices ρ_{Fv} (for monthly returns, it is 16.5% for TS09, and smaller than 10% for our model (both sub-specifications); for daily returns, it is around 10% for both models), implying the large extent to which volatility is unspanned by the futures contracts. As indicated in Chiarella et al. (2013), volatility risk of a volatility factor with null correlation cannot be spanned by futures contracts. Therefore, we show it is also important in the natural gas derivatives market.

In the commodity price literature, Nomikos and Andriosopoulos (2012), Kristoufek (2014), and Baum et al. (2021) find an ILE or positive price-variance correlation coefficient ρ_{Sv} or ρ_{Fv} in the natural gas market (that is, volatility becomes higher when energy returns increase). ILE arises because positive shocks have a much more pronounced effect on futures dynamics than negative shocks. As pointed out in Benth and Vos (2013), it occurs when the volatility tends to increase with the level of power prices because of the negative relationship between inventories and prices: the smaller the inventories level, the higher the price volatility.

San17 considers jumps an important feature of spot returns of the HH spot prices and propose a model with mean-reversion and stochastic jump intensity linked to the temperature. According to BLW18, spikes are important for explaining forward prices in the UK natural gas market. From Figs. 3 and 4 we can see that there are jumps in prices in both directions. Baum et al. (2021) indicate that these shocks in prices, positive and negative, can be seen as

a consequence of market deregulation or as a result of the financialisation of this particular market.

Several papers explicitly account for a mean-reversion in the gas spot price; this is the case of, e.g., EG98, San17 and BLW18. Alternatively, and since recent studies show that there is no significant mean-reversion in oil prices, it is not needed to explicitly model it, as it is the case of TS09. The model we propose in our original set-up indirectly accounts for this mean-reversion through the parameter ρ_{Sy}, negative and unitary in our case: it is achieved when prices go up due to an increase in the cost of carry (decrease in the convenience yield), as can be observed from Eq. (2.1). However, and since we are focused on futures prices under the $\mathbb{Q}$ measure, this mean-reversion in spot prices is trivial due to the martingale condition. In case one wanted to incorporate it in the model, one would have to seek for an additional term which cancels out the futures' dynamics drift term. Therefore, we do not incorporate this feature in our model.

3.3 Parameters estimation

The inputs to the calibration algorithm consist of the underlying futures prices, option strikes and discount factors. Additionally, and as a proxy for the instantaneous variance v_t, we use squared ATM volatilities which correspond to the shortest available maturity contract (in our case, the contracts labeled M2 or M3)—that is, a unique variance value per observation date. We use a least-squares fitting with the objective of minimising the root mean squared error in volatilities RMSE(σ). With the calibrated parameters and for comparative purposes, we also report mean absolute errors MAE(σ) in option volatilities.

We apply Feller's condition to all models with stochastic volatility, that is, all models considered except Mer76. Hes93 and Bat96 assume that $\sigma_S = 1$; following this assumption, we also assume that $\sigma_S = 1$ in TS09-SV1 and our model in the original set-up, $\sigma_S = 0$ in the alternative set-up. We calibrate the parameters for the models listed in Sect. 2.2.1 and for our model.

We define our model dynamics directly under $\mathbb{Q}$, therefore the parameter estimation is performed under this measure. Subject to the original characterisation of the parameters, the 10 parameters in our model are $\Phi \equiv \{\sigma_S, \alpha, \gamma, \kappa, a^\theta, b^\theta, c^\theta, \rho_{Sy}, \rho_{Sv}, \rho_{yv}\}$, whereas conditional to the alternative set-up, the 8 parameters are $\Phi \equiv \{\alpha_0, \alpha, \gamma, \kappa, a^\theta, b^\theta, c^\theta, \rho_{Fv}\}$. In this work we study the empirical pricing performance of the models using the least-squares estimation method, under which the procedure to obtain the parameter estimates $\Phi^\star$ for every observation date t is defined as

$$\Phi^\star = \underset{\Phi}{\arg\min}\, MAE_t^\sigma (\Phi) = \underset{arg\,min}{\Phi}\, \frac{1}{N} \sum_{i=1}^{N} \left| \hat{\sigma}_{t,i}(\Phi) - \sigma_{t,i} \right|, \tag{3.1}$$

$$\Phi^\star = \underset{\Phi}{\arg\min}\, RMSE_t^\sigma (\Phi) = \underset{arg\,min}{\Phi}\, \sqrt{\frac{1}{N} \sum_{i=1}^{N} \left(\hat{\sigma}_{t,i}(\Phi) - \sigma_{t,i} \right)^2}, \tag{3.2}$$

where $\sigma_{t,i}$ is the observed market volatility of option i out of N used for the estimation at time t, and $\hat{\sigma}_{t,i}(\Phi)$ is the theoretical model volatility based on a set of parameters. We compute implied volatilities employing the standard model of Black (1976). Parameters are not allowed to take values that are inconsistent with the model framework. Disregarding the seasonality, the following restrictions are applied for the original set-up: $\sigma_S = 1; \alpha, \gamma, \kappa, \sigma_v > 0; \rho_{Sy}, \rho_{Sv}, \rho_{yv} \in (-1, 1)$; for the alternative set-up: $\alpha =$

Table 6 R^2 analysis

(a) R^2 per peak, years 2011–2020

R^2	1/12	2/12	3/12	4/12	5/12	6/12	7/12	8/12	9/12	10/12	11/12	12/12
S	0.66%	0.22%	2.63%	5.47%	5.95%	3.55%	0.66%	0.22%	2.63%	**5.95%**	5.47%	3.55%
$M(b^\theta = 0)$	5.47%	5.95%	3.55%	0.66%	0.22%	2.63%	5.47%	5.95%	3.55%	**0.22%**	0.66%	2.63%
M	6.15%	6.15%	6.15%	6.15%	6.15%	6.15%	6.15%	6.15%	6.15%	**6.15%**	6.15%	6.15%

(b) R^2 per year, peak $t_0 = 10/12$

R^2	2011	2012	2013	2014	2015	2016	2017	2018	2019	2020	All
S	0.08%	58.76%	7.13%	43.48%	10.09%	1.95%	38.21%	28.73%	**79.12%**	0.67%	5.95%
$M(b^\theta = 0)$	9.96%	14.60%	6.84%	12.66%	41.60%	38.19%	27.74%	9.42%	**6.38%**	23.00%	0.22%
M	10.01%	74.89%	14.16%	58.85%	52.51%	40.48%	66.93%	38.59%	**84.85%**	23.53%	6.15%

(c) R^2 per peak, years 2011–2020—averaged values

R^2	1/12	2/12	3/12	4/12	5/12	6/12	7/12	8/12	9/12	10/12	11/12	12/12
S	1.78%	23.49%	49.85%	54.40%	32.79%	6.43%	1.78%	23.49%	49.85%	**54.40%**	32.79%	6.43%
$M(b^\theta = 0)$	54.50%	32.79%	6.43%	1.78%	23.49%	49.85%	54.50%	32.79%	6.43%	**1.78%**	23.49%	49.85%
M	56.28%	56.28%	56.28%	56.28%	56.28%	56.28%	56.28%	56.28%	56.28%	**56.28%**	56.28%	56.82%

These tables present the values of R^2 calculated when regressing the series of ATM market variance v_t (squared of the quoted volatility) for the shortest futures contract available (in this case, M3) in terms of a cosinus and/or sinus functions. Sub-table (a) considers the whole sample period 2011–2020 and checks the effect of each month as peak of the volatility series. Sub-table (b) considers each year individually in the whole sample period and checks the effect of $t_0 = 10/12$ as peak of the series. Sub-table (c) considers the whole sample period and all the contracts, and checks the effect of each month as peak of the series, on variance values averaged by trade month. With $M(b^\theta = 0)$ we refer to a new simple pattern based only on the sinus. In all sub-tables and in bold we highlight those cases which present higher R^2 values for the simple sinusoidal pattern S

Table 7 MAE(σ) analysis

$MAE(\sigma)$	1/12	2/12	3/12	4/12	5/12	6/12	7/12	8/12	9/12	10/12	11/12	12/12
Ø	4.34%	4.34%	4.34%	4.34%	4.34%	4.34%	4.34%	4.34%	4.34%	**4.34%**	4.34%	4.34%
S	4.35%	4.33%	4.28%	4.26%	4.29%	4.34%	4.33%	4.33%	4.29%	**4.26%**	4.29%	4.33%
M	4.28%	4.31%	4.28%	4.25%	4.25%	4.26%	4.28%	4.31%	4.28%	**4.25%**	4.25%	4.26%

This table presents MAE(σ) errors performed by our model, calculated when regressing the series of ATM market variance v_t (squared of the quoted volatility) for the shortest futures contract available (in this case, M3) in terms of a cosinus and/or sinus functions. We use the symbol Øto identify the lack of seasonality in the variance v_t, this is equivalent to a constant θ_t parameter, namely the TS09-SV1 model. In bold we highlight those cases which present smaller error values for the simple sinusoidal pattern S

1; $\alpha_0, \gamma, \kappa, \sigma_v > 0$; $\rho_{Fv} \in (-1, 1)$. Furthermore, the parameters governing the seasonality are restricted to ensure their uniqueness: $a^\theta > 0$, $a^\theta \geq |b^\theta|$, $a^\theta \geq |c^\theta|$ and $t_0 \in [0, 1[$, with January 1st representing the time origin. We define the values t_0 can get discretising the year on a monthly basis, that is, $t_0 = 1/12, 2/12, \dots, 12/12$. Observe that the parameter t_0 is not included in the vector Φ since its value is assigned in advanced. A detailed description of how we decide the value of the peak t_0 can be found in Sect. 4 (paragraph "Deciding the Value for the Seasonal Peak"), together with Tables 6 and 7.

3.3.1 Interpretation of the parameters' estimates

In Table 8 we present the estimated parameters, errors and computation times we obtain by solving Eqs. (3.1) and (3.2). We perform two sets of analyses, each of which considers different frequency in the market data—monthly and daily. Below we interpret the values obtained for the parameters' estimates. In line with the stylised facts in the gas market introduced in Sects. 1 and 3.2, we provide evidence that our model accounts for a series of properties, such as mean-reversion and jumps in prices, seasonality in prices and in volatilities, ILE and the Samuelson effect.

We observe that the estimated correlation coefficients between prices and volatilities, ρ_{Sv} and ρ_{Fv}, for each model considered (except for Bat96) are positive and quite close between them. As we have already discussed in Sect. 3.2, and in line with Kristoufek (2014) and Baum et al. (2021), this represents the evidence of the ILE in the natural gas market. However, this finding is in contrast with the distribution of futures returns in Figs. 3a, b, where we can observe increasing volatilities coinciding also with highly negative returns. We think that since we find an ILE but also there are negative jumps in prices, there is a justification for the incorporation of jumps in this model for this particular market.

We find that the correlations between the remaining pairs of factors ρ_{Sy} and ρ_{yv} are negative; the first equals the unity indicating a clear mean-reversion pattern in spot prices, and the latter, which value is quite close to that of ρ_{Sy} but of contrary sign, is also in line with this mean-reversion.

With regards to the cost of carry volatility parameters in Eq. (2.4), we highlight that the damping factor γ is of large magnitude in the original set-up (larger than 10), and almost zero in the alternative one—the latter is in line with the results obtained in TS09. In the alternative set-up, we fix the scaling factor α to one, in the alternative one the calibrated value is around 1.5.

In terms of the parameters associated to the variance factor, we obtain very large values for the speed of mean-reversion κ in the original set up (around 18 for the simple, around 20 for the multiple pattern), whereas the value is around 1.5 in the alternative case. And on the contrary, the long-run mean-reversion level θ^a is larger in the alternative set-up than in the original one, showing smaller magnitude of oscillations around this level through the effect of the new parameters θ^b and θ^c.

4 Results

In this section we implement our novel term-structure model SSYSV described in Sects. 2 and 2.3, which displays stochastic spot prices and forward cost of carry curves (equivalent to stochastic futures prices) as well as SSV. For a panel of models, we calibrate their parameters for pricing ATM and OTM options, spanning different strikes and maturities, over a time period of exactly 10 years. The results are obtained using analytical expressions for the CF of the futures log-prices. Following Carr and Madan (1999), we use Simpson's rule to calculate the integral in the pricing functions (2.37) and (2.38) numerically, for which we use Matlab's built-in function *simps*. We use a standard fourth order Runge-Kutta algorithm to solve the system of ODEs (2.22)-(2.23), for which we use Matlab's built-in function *ode*45. We consider an integral step of 1/10 and an upper bound of 60, which implies 600 evaluation points. We set the value of the control parameter α to 0.75. The experiments are implemented in a HP laptop computer configured with an Intel Core i7 2.60 GHz 16 GB RAM and SSD

Table 8 Estimated parameters, errors and computation time

(a) Monthly observations

Model	SYSSV				ST21	ST18	TS09-SV1		Bat96	Hes93	Mer76
Seasonality	Multiple		Simple						✓		
Set-up	★	✓	★	✓			★	✓			
σ_S	–	1.0000	–	1.0000	–	–	–	1.0000	–	–	0.2591
α_0	1.5886	–	1.4311	–	–	–	2.4336	–	–	–	–
α	1.0000	1.5454	1.0000	1.5438	–	–	1.0000	1.5144	–	–	–
γ	22.9148	0.2921	13.9186	0.4525	1.2394	1.2475	18.6119	0.2804	–	–	–
κ	17.7878	1.1011	15.1016	1.1192	2.4543	2.4879	40.4542	1.2827	5.8069	5.6512	–
a^{θ},θ	0.0276	0.5168	0.0335	0.5028	0.2294	0.2289	0.0100	0.4486	0.0152	0.0774	–
b^{θ}	0.0037	0.0007	0.0039	0.0013	–0.0070	–	–	–	–	–	–
c^{θ}	0.0018	–0.0002	–	–	–	–	–	–	–	–	–
σ_v	0.9916	0.5532	0.9175	0.5697	0.3308	0.2630	0.7934	0.5754	0.1375	0.0689	–
ρ_{Sy}	–	–1.0000	–	–1.0000	–	–	–	–1.0000	–	–	–
ρ_{Sv}	–	0.1144	–	0.1042	–	–	–	0.2191	–1.0000	0.9999	–
ρ_{yv}	–	–0.1300	–	–0.1092	–	–	–	–0.3845	–	–	–
ρ_{Fv}	0.0872	–	0.0972	–	0.1800	0.2242	0.1647	–	–	–	–
λ	–	–	–	–	–	–	–	–	5.3309	5.6512	5.9153
μ_J	–	–	–	–	–	–	–	–	0.0451	0.0774	0.0737
σ_J	–	–	–	–	–	–	–	–	0.0803	–	0.0013
Count	9	11	8	10	6	5	7	9	7	4	4
MAE(σ)	0.0416	0.0425	0.0420	0.0426	0.0434	0.0436	0.0433	0.0434	0.0432	0.0480	0.0766
RMSE(σ)	0.0586	0.0596	0.0591	0.0597	0.0607	0.0608	0.0600	0.0605	0.0611	0.0657	0.1002
ACT	0.1474	0.1567	0.1149	0.0785	0.0394	0.0639	0.1219	0.1108	0.6661	0.0981	0.2204

Table 8 continued

	SYSSV				ST21	ST18	TS09-SV1		Bat96	Hes93	Mer76
	(b) Daily observations										
Model	SYSSV				ST21	ST18	TS09-SV1		Bat96	Hes93	Mer76
Seasonality	Multiple		Simple								
Set-up	★	✓	★	✓			★	✓			
σ_S	–	1.0000	–	1.0000	–	–	–	1.0000	–	–	0.2826
α_0	1.8058	–	1.4354	–	–	–	1.5586	–	–	–	–
α	1.0000	1.4060	1.0000	1.4268	1.2230	1.2598	1.0000	1.4082	–	–	–
γ	24.7212	0.4387	21.2379	0.2795	–	–	24.0451	0.2953	–	–	–
κ	21.4165	13.9554	1.2444	1.2389	2.1558	2.1077	16.1562	1.3894	5.6808	5.8078	–
a^θ, θ	0.0197	0.4190	0.0349	0.4507	0.3013	0.3435	0.0284	0.4150	0.0300	0.0893	–
b^θ	0.0018	–0.0000	0.0012	0.0002	–0.0095	–	–	–	–	–	–
c^θ	0.0023	–0.0003	–	–	–	–	–	–	–	–	–
σ_v	0.9191	0.5383	0.9870	0.6194	0.2579	0.2923	0.9548	0.6638	0.2324	0.0769	–
ρ_{Sy}	–	0.0240	–	0.0865	–	–	–	0.1214	–	–	–
ρ_{Sv}	–0.9999	–	–0.9991	–	–	–	–0.9994	–	–1.0000	0.9987	–
ρ_{yv}	–	–0.0184	–	–0.1076	–	–	–	–0.1875	–	–	–
$\rho_{\Gamma v}$	–	0.1079	–	0.0918	0.1962	0.2471	–	0.0976	–	–	–
λ	–	–	–	–	–	–	–	–	1.1827	–	2.0685
μ_J	–	–	–	–	–	–	–	–	0.1816	–	0.1149
σ_J	–	–	–	–	–	–	–	–	0.0352	–	0.0000
Count	9	11	8	10	6	5	7	9	7	4	4
MAE(σ)	0.0437	0.0438	0.0442	0.0443	0.0445	0.0446	0.0442	0.0444	0.0439	0.0463	0.0670
RMSE(σ)	0.0620	0.0625	0.0625	0.0625	0.0626	0.0627	0.0624	0.0626	0.0632	0.0660	0.0950
ACT	3.8576	5.9236	2.0122	2.0370	0.7694	0.6831	1.1509	1.1935	9.0950	2.3092	4.6260

We set the peak value $t_0 = 10/12$ (end of October) in ST21 and SYSSV. MAE(σ) represents the mean absolute pricing error in option volatilities. RMSE(σ) represents the square root of the quadratic mean of errors in option volatilities. The pricing errors are defined as the differences between fitted volatilities $\hat{\sigma}_t$ and market implied (Black) volatilities σ_t. Count refers to the number of parameters. ACT refers to the computation time using analytical solutions; values are expressed in hours

hard drive, running Windows 10 64 bits, Matlab version R2020b 64 bits and Microsoft Office 365 64 bits.

Deciding the Value for the Seasonal Peak

We fix the value of the peak parameter t_0 based on the evidence of the seasonal behaviour of the HH natural gas futures' prices. To correctly determine its value, we consider two different alternatives which we describe in the following paragraph. For both alternatives, we find that the peak corresponds to $t_0 = 10/12$, that is, end of October.

One way consists of analysing the implied ATM Black volatility data observing the whole sample period. We then regress a sinusoidal function depending on the 12 values t_0 can get to determine which one delivers the highest R^2. Due to the Samuelson effect (see Fig. 2a, $R^2 = 97.19\%$), we consider it is enough to select one single contract to do so, M3,[13] instead of all the contracts taken together. A detailed description of this alternative can be found in the paragraph below, together with the information displayed in Tables 6 and 7. Another way consists of carrying out a similar exercise, this time averaging the contracts by trading month; this results can be observed in Fig. 2b. Per each of the 12 values of t_0, we calculate an average of all available ATM volatilities; these values correspond to the blue dots. We then regress a sinusoidal function seeking the value for t_0 which delivers the highest R^2; these values correspond to the red line.

Table 6 presents the values for the coefficient R^2 when regressing the market variance v_t in terms of three different sinusoidal patterns: S refers to the original simple pattern based on the cosinus function; $M(b^\theta = 0)$ refers to an alternative simple pattern based on the sinus function; M refers to the original mixed pattern. Table 6a already considers the whole period 2011–2020 and checks the effect in R^2 for each value t_0 can get. To calculate R^2, we consider all the implied variances for the contract M3 for the whole period. For S, the best results are obtained when $t_0 = 10/12$ ($R^2 = 5.95\%$) and, as we anticipated for M, all values perform equally. There is a clear explanation for such a small value of R^2 when considering the whole time series, as we did not isolate other economic factors from the analysis such as economic news or a trend in v_t. Table 6b considers $t_0 = 10/12$ as the peak and checks the effect in R^2 for each year in the sample period, and all the years taken together. To calculate R^2, we consider all the implied variances for the contract M3. The value for R^2 is clearly larger for M, which allows us to identify what years adjust best. Some years present a very good fit, such as 2012 ($R^2 = 74.89\%$) and 2019 ($R^2 = 84.85\%$); other years display a very poor performance, it is the case of 2011 ($R^2 = 10.01\%$) and 2013 ($R^2 = 14.16\%$). We think that the reason behind these differences is that, in certain years and as previously indicated, there are other facts which clearly affect the variance that are not taken into consideration. Observe that taking all years together delivers the same values obtained in the previous sub-table. Finally we carry out an additional analysis in Table 6c, where we average variances per trading month, considering the whole sample period and all the contracts. We check again the effect of each month as peak of the variance series, but following a different perspective. Again, we find that the best performance in terms of R^2 corresponds to October (54.40% for S, 56.28% for M). In complement to this, in Fig. 2b we present these averaged values and the correspondent regression on market variance, assuming a single harmonic pattern. Using $t_0 = 10/12$ and for the panel of models, the calibrated parameters and correspondent error statistics can be found in Table 8. Additionally and following the results in Table 6b, we perform an equivalent analysis based on the best two individual years (2019 and 2020) for which results are reported in Table 9.

---

[13] We have not chosen the shorter maturity contract M2 due to the lack of many ATM volatility values in the sample period, especially during the first half of it.

Table 9 Estimated parameters, errors and computation time – monthly observations, single years

(a) 2019

Model	SYSSV				ST21	ST18	TS09-SV1		Bat96	Hes93	Mer76
Seasonality	Multiple		Simple								
Set-up	★	✓	★	✓	★	★	★	✓			
σ_S	–	1.0000	–	1.0000	–	–	–	1.0000	–	–	0.2697
α_0	1.6432	–	1.5596	–	–	–	2.0264	–	–	–	–
α	1.0000	1.4298	1.0000	1.5470	–	–	1.0000	1.6168	–	–	–
γ	13.7456	0.3180	15.3799	0.3035	1.3576	1.4247	33.1492	0.3769	–	–	–
κ	19.7671	1.7262	17.9145	1.3992	2.5633	2.6944	26.9385	1.7346	6.8128	6.5113	–
a^θ, θ	0.0203	0.3175	0.0234	0.3936	0.2095	0.2168	0.0121	0.3478	0.0001	0.0661	–
b^θ	0.0027	0.0004	0.0032	0.0008	−0.0088	–	–	–	–	–	–
c^θ	0.0010	−0.0005	–	–	–	–	–	–	–	–	–
σ_v	0.8159	0.6970	0.9048	0.6954	0.7529	0.8017	0.6763	0.7550	0.0831	0.0733	–
ρ_{Sy}	–	−1.0000	–	−1.0000	–	–	–	−1.0000	–	–	–
ρ_{Sv}	–	0.0768	–	0.1028	–	–	–	0.1104	1.0000	0.7453	–
ρ_{yv}	–	−0.1668	–	−0.1999	–	–	–	−0.2431	–	–	–
ρ_{Fv}	0.1158	–	0.1013	–	0.0656	0.0657	0.1491	–	–	–	–
λ	–	–	–	–	–	–	–	–	3.1753	–	0.4189
μ_J	–	–	–	–	–	–	–	–	−0.0102	–	0.1473
σ_J	–	–	–	–	–	–	–	–	0.1304	–	0.0009
Count	9	11	8	10	6	5	7	9	7	4	4
MAE(σ)	0.0537	0.0536	0.0540	0.0549	0.0542	0.0544	0.0540	0.0544	0.0561	0.0601	0.0790
RMSE(σ)	0.0679	0.0677	0.0681	0.0686	0.0698	0.0697	0.0689	0.0691	0.0709	0.0766	0.1052
ACT	0.0104	0.1781	0.0151	0.2136	0.0142	0.0130	0.0098	0.0754	0.0373	0.0182	0.0161

Table 9 continued

	(b) 2020										
Model	SYSSV				ST21	ST18	TS09-SV1		Bat96	Hes93	Mer76
Seasonality	Multiple		Simple								
Set-up	★	✓	★	✓		★	★	✓			
σ_S	—	1.0000	—	1.0000	—	—	—	1.0000	—	—	0.3672
α_0	1.4472	—	1.3812	—	—	—	1.4591	—	—	—	—
α	1.0000	1.4651	1.0000	1.4677	—	—	1.0000	1.2039	—	—	—
γ	15.1775	0.5065	20.6621	0.5008	1.0145	0.9789	14.3886	0.2657	—	—	—
κ	14.3425	0.9107	12.7726	0.9857	2.0569	1.9654	10.0686	1.7874	4.4405	3.2484	—
a^θ, θ	0.0398	0.6223	0.0427	0.6390	0.2170	1.1986	0.0121	0.3501	0.0010	0.0161	—
b^θ	0.0105	0.0061	0.0037	0.0066	−0.0279	—	—	—	—	—	—
c^θ	0.0018	−0.0010	—	—	—	—	—	—	—	—	—
σ_v	0.3793	0.4924	0.0500	0.5079	0.1330	0.1562	0.0836	0.5801	0.0515	0.0749	—
ρ_{Sy}	—	−0.9992	—	−0.9998	—	—	—	−0.9979	—	—	—
ρ_{Sv}	—	0.0204	—	0.0379	—	—	—	0.1399	0.7723	0.9998	—
ρ_{yv}	—	0.0045	—	0.0147	—	—	—	−0.2782	—	—	—
ρ_{Fv}	0.2465	—	0.2249	—	0.5812	0.5417	0.9998	—	—	—	—
λ	—	—	—	—	—	—	—	—	7.0755	—	7.3694
μ_J	—	—	—	—	—	—	—	—	0.0762	—	0.0712
σ_J	—	—	—	—	—	—	—	—	0.0018	—	0.0009
Count	9	11	8	10	6	5	7	9	7	4	4
MAE(σ)	0.0543	0.0540	0.0538	0.0548	0.0577	0.0588	0.0554	0.0573	0.0601	0.0639	0.1052
RMSE(σ)	0.0684	0.0696	0.0681	0.00704	0.0757	0.0765	0.0701	0.0750	0.0766	0.0822	0.1276
ACT	0.0107	0.2723	0.0155	0.2736	0.0112	0.0154	0.0126	0.0754	0.0481	0.0188	0.0215

We set the peak value $t_0 = 10/12$ (end of October) in ST21 and SYSSV. MAE(σ) represents the mean absolute pricing error in option volatilities, RMSE(σ) represents the square root of the quadratic mean of errors in option volatilities. The pricing errors are defined as the differences between fitted volatilities $\hat{\sigma}_t$ and market implied (Black) volatilities σ_t. Count refers to the number of parameters. ACT refers to the computation time using analytical solutions; values are expressed in hours

Table 7 presents the values for the error estimates MAE(σ) in the case we perform the calibration on each peak value, for our benchmark (Ø) and our model specifications (S, M). Regarding our model and no matter what specification we pick, we can observe that the smallest errors are obtained when we consider October the peak (4.26% and 4.25%, correspondingly). Results in Table 7 are, then, in line with those in Table 6. These analyses are performed using the original characterisation of the parameters. Similar results are obtained using the alternative set-up.[14]

Interpreting the Pricing Errors
Based on $t_0 = 10/12$ and for the period described in Sect. 3, our calibration results are reported in Table 8. We perform two sets of analysis: Sub-table (a) considers monthly data, Sub-table (b) focuses on daily data. For each model considered, we display the parameters' estimates, the pricing errors MAE(σ) and RMSE(σ), and the computation times. Under the original (alternative) set-up, the average MAE(σ) for our model is 4.18% (4.25%), this is a 0.15% (0.09%) less than TS09-SV1,[15] almost identical error values. Lastly, we carry out a transverse analysis of the errors' distribution between our model and TS09-SV1, seeking for a pattern.

Next we compare model performances based on the monthly data set by means of the MAE(σ) estimates. In an aggregated level, the overperformance of our model compared to the benchmark, displayed in Table 8, does not seem to be quite large. Tables 10 and 11 (12 and 13) follow the original (alternative) characterisation of the parameters and present the disaggregated structure of the errors. Sub-tables (a) display the errors using the benchmark model TS09-SV1; Sub-tables (b) display the errors using our model, following sub-specifications S and M respectively. Both models perform worst (that is, present larger errors) for shorter maturity contracts, after which the model performance improves for both. Sub-tables (c) display the difference in errors between both models, with larger values indicating that our model outperforms the benchmark. In this sub-table we observe the most significant improvement, specifically (i) for deeper OTM options, particularly puts in shorter maturity contracts (i.e., M2 and M3) dealing with the original set-up; and (ii) for closer-to-the-ATM options, particularly puts in the very short maturity contracts (i.e., M2) when we deal with the alternative set-up, where improvement reaches 3.5%. For longer maturity contracts, both models display similar performance. The results we obtain for the alternative set-up deserve a closer analysis, since the benefit of using our model is quite large, specially for shorter contracts. We find that our model clearly outperforms the benchmark for short maturities, specially for those options closer to the ATM level, reaching a 3.6% with the simple S pattern and a 3.5% with the mixed M one. For M2 only, our model outperforms the benchmark on average in 1.3% and 1.9%, respectively.

In our panel we also include two very recent models on futures dynamics, one without and one with seasonality in the variance, they are ST18 and ST21. In an aggregated level, the improvement displayed in Table 8 does not seem to be quite large. In Table 14 we compare the errors' structure in ST21 with that in the alternative set-up version of our model SYSSV^S, with identical seasonality specification (that is, the simple S one). We find that our model clearly outperforms the benchmark for short maturities, specially for deep-OTM put options, reaching a 3.1% for the shortest maturity contract (i.e., M2) and the deeper-OTM put options. For M2 only and on average, our model outperforms ST21 in 0.8%.

---

[14] The proof is available by direct request to the authors.

[15] Our model consists of an extension of TS09-SV1, therefore we compare both performances.

Table 10 MAE(σ)—simple harmonic pattern and original set-up

MAE(σ)	(a) TS09-SV1								(b) SYSSV^S								(c) Diff. TS09-SV1 − SYSSV^S							
	M2	M3	M4	M5	M6	M7	M8	ALL	M2	M3	M4	M5	M6	M7	M8	ALL	M2	M3	M4	M5	M6	M7	M8	ALL
p − 7.5	0.0798	0.0557	0.0502	0.0487	0.0424	0.0345	0.0328	0.0492	0.0750	0.0497	0.0488	0.0488	0.0422	0.0337	0.0325	0.0472	0.0048	0.0059	0.0014	−0.0001	0.0002	0.0008	0.0003	0.0019
p − 7	0	0.0540	0.0504	0.0459	0.0425	0.0351	0.0337	0.0436	0	0.0474	0.0479	0.0459	0.0425	0.0341	0.0326	0.0417	0	0.0067	0.0025	0.0000	0.0000	0.0010	0.0010	0.0019
p − 6.5	0	0.0498	0.0486	0.0478	0.0420	0.0353	0.0327	0.0427	0	0.0464	0.0466	0.0479	0.0421	0.0347	0.0320	0.0416	0	0.0033	0.0020	0.0000	−0.0001	0.0007	0.0007	0.0011
p − 6	0	0.0501	0.0483	0.0483	0.0447	0.0364	0.0327	0.0434	0	0.0465	0.0466	0.0485	0.0446	0.0357	0.0315	0.0422	0	0.0037	0.0017	−0.0002	0.0001	0.0006	0.0012	0.0012
p − 5.5	0	0.0451	0.0478	0.0470	0.0440	0.0342	0.0320	0.0417	0	0.0418	0.0459	0.0473	0.0440	0.0334	0.0309	0.0405	0	0.0033	0.0020	−0.0003	0.0000	0.0008	0.0012	0.0012
p − 5	0.0657	0.0445	0.0462	0.0465	0.0436	0.0340	0.0326	0.0447	0.0527	0.0414	0.0445	0.0464	0.0437	0.0333	0.0313	0.0419	0.0130	0.0031	0.0016	0.0001	−0.0001	0.0007	0.0012	0.0028
p − 4.5	0.0937	0.0427	0.0451	0.0453	0.0457	0.0345	0.0317	0.0466	0.0870	0.0399	0.0433	0.0460	0.0459	0.0336	0.0308	0.0466	0.0068	0.0028	0.0018	−0.0007	−0.0002	0.0009	0.0009	0.0018
p − 4	0.0532	0.0420	0.0444	0.0475	0.0438	0.0345	0.0316	0.0424	0.0460	0.0391	0.0425	0.0481	0.0442	0.0337	0.0303	0.0406	0.0072	0.0029	0.0019	−0.0006	−0.0004	0.0008	0.0014	0.0019
p − 3.5	0.0463	0.0410	0.0445	0.0464	0.0454	0.0343	0.0319	0.0414	0.0416	0.0382	0.0430	0.0471	0.0455	0.0334	0.0310	0.0400	0.0047	0.0028	0.0015	−0.0006	0.0000	0.0009	0.0010	0.0015
p − 3	0.0424	0.0398	0.0437	0.0473	0.0457	0.0353	0.0314	0.0408	0.0395	0.0372	0.0421	0.0475	0.0457	0.0344	0.0305	0.0396	0.0029	0.0026	0.0016	−0.0003	0.0000	0.0008	0.0009	0.0012
p − 2.5	0.0397	0.0389	0.0438	0.0478	0.0457	0.0358	0.0320	0.0405	0.0373	0.0362	0.0426	0.0479	0.0460	0.0349	0.0312	0.0395	0.0024	0.0027	0.0012	−0.0001	−0.0003	0.0008	0.0008	0.0011
p − 2	0	0.0372	0.0435	0.0472	0.0465	0.0337	0.0321	0.0400	0	0.0346	0.0420	0.0476	0.0467	0.0329	0.0310	0.0391	0	0.0026	0.0015	−0.0003	−0.0002	0.0008	0.0010	0.0009
p − 1.5	0.0388	0.0374	0.0444	0.0489	0.0494	0.0352	0.0327	0.0410	0.0359	0.0350	0.0431	0.0494	0.0497	0.0344	0.0319	0.0399	0.0030	0.0024	0.0013	−0.0005	−0.0003	0.0008	0.0008	0.0011
p − 1	0.0604	0.0367	0.0446	0.0491	0.0473	0.0375	0.0325	0.0440	0.0558	0.0344	0.0436	0.0495	0.0477	0.0369	0.0316	0.0428	0.0046	0.0024	0.0009	−0.0004	−0.0005	0.0006	0.0008	0.0012
p − 0.5	0.0378	0.0361	0.0443	0.0489	0.0480	0.0363	0.0318	0.0405	0.0345	0.0341	0.0436	0.0482	0.0482	0.0356	0.0311	0.0395	0.0034	0.0020	0.0008	−0.0004	−0.0001	0.0007	0.0007	0.0010
p − 0	0.0369	0.0354	0.0432	0.0472	0.0471	0.0351	0.0305	0.0393	0.0338	0.0333	0.0423	0.0475	0.0474	0.0345	0.0305	0.0385	0.0031	0.0021	0.0009	−0.0003	−0.0003	0.0006	0.0001	0.0009
c − 0	0.0371	0.0363	0.0445	0.0483	0.0471	0.0359	0.0324	0.0402	0.0338	0.0343	0.0439	0.0487	0.0473	0.0351	0.0319	0.0393	0.0034	0.0021	0.0006	−0.0004	−0.0002	0.0008	0.0005	0.0010
c − 0.5	0	0.0351	0.0430	0.0481	0.0476	0.0373	0.0315	0.0404	0	0.0331	0.0421	0.0486	0.0479	0.0366	0.0314	0.0400	0	0.0020	0.0008	−0.0006	−0.0003	0.0007	0.0008	0.0005
c − 1	0	0.0351	0.0434	0.0486	0.0481	0.0383	0.0317	0.0409	0	0.0333	0.0423	0.0491	0.0484	0.0377	0.0315	0.0405	0	0.0019	0.0006	−0.0005	−0.0003	0.0006	0.0002	0.0004
c − 1.5	0	0.0354	0.0434	0.0480	0.0481	0.0379	0.0323	0.0409	0	0.0339	0.0430	0.0486	0.0486	0.0374	0.0321	0.0406	0	0.0016	0.0005	−0.0005	−0.0005	0.0006	0.0001	0.0003
c − 2	0	0.0354	0.0442	0.0496	0.0490	0.0384	0.0325	0.0415	0	0.0341	0.0439	0.0503	0.0494	0.0379	0.0324	0.0413	0	0.0013	0.0003	−0.0008	−0.0003	0.0005	0.0001	0.0002
c − 2.5	0	0.0357	0.0442	0.0496	0.0501	0.0378	0.0337	0.0418	0	0.0346	0.0438	0.0505	0.0505	0.0374	0.0336	0.0417	0	0.0011	0.0003	−0.0009	−0.0004	0.0004	0.0001	0.0001
c − 3	0	0.0362	0.0447	0.0503	0.0499	0.0397	0.0342	0.0425	0	0.0353	0.0446	0.0512	0.0503	0.0393	0.0340	0.0425	0	0.0009	0.0001	−0.0009	−0.0004	0.0004	0.0003	0.0000
c − 3.5	0.0577	0.0368	0.0447	0.0502	0.0514	0.0389	0.0348	0.0449	0.0568	0.0361	0.0447	0.0510	0.0518	0.0387	0.0343	0.0448	0.0010	0.0007	0.0001	−0.0008	−0.0004	0.0002	0.0004	0.0002
c − 4	0	0.0369	0.0451	0.0519	0.0519	0.0405	0.0350	0.0436	0	0.0364	0.0452	0.0528	0.0523	0.0404	0.0345	0.0436	0	0.0005	−0.0001	−0.0009	−0.0004	0.0002	0.0002	−0.0001
c − 4.5	0.0605	0.0371	0.0452	0.0521	0.0529	0.0412	0.0351	0.0463	0.0600	0.0367	0.0452	0.0530	0.0533	0.0409	0.0349	0.0463	0.0005	0.0004	0.0000	−0.0009	−0.0004	0.0003	0.0002	0.0000
c − 5	0.0623	0.0375	0.0458	0.0513	0.0533	0.0411	0.0359	0.0467	0.0616	0.0373	0.0464	0.0524	0.0536	0.0411	0.0354	0.0468	0.0007	0.0002	−0.0006	−0.0012	−0.0003	0.0000	0.0005	−0.0001
c − 5.5	0	0.0380	0.0463	0.0520	0.0536	0.0424	0.0374	0.0450	0	0.0380	0.0471	0.0530	0.0540	0.0422	0.0369	0.0452	0	0.0000	−0.0008	−0.0010	−0.0004	0.0002	0.0005	−0.0003
c − 6	0.0567	0.0387	0.0466	0.0532	0.0559	0.0433	0.0372	0.0474	0.0558	0.0388	0.0475	0.0546	0.0565	0.0432	0.0368	0.0476	0.0009	−0.0001	−0.0009	−0.0014	−0.0006	0.0001	0.0003	−0.0002
c − 6.5	0	0.0386	0.0472	0.0524	0.0556	0.0426	0.0371	0.0456	0	0.0388	0.0482	0.0524	0.0560	0.0424	0.0366	0.0460	0	−0.0002	−0.0010	−0.0014	−0.0005	0.0002	0.0005	−0.0004
c − 7	0	0.0389	0.0466	0.0524	0.0552	0.0438	0.0386	0.0463	0	0.0391	0.0477	0.0559	0.0556	0.0435	0.0382	0.0467	0	−0.0002	−0.0011	−0.0014	−0.0004	0.0003	0.0005	−0.0004
c − 7.5	0.0671	0.0396	0.0478	0.0532	0.0557	0.0459	0.0387	0.0497	0.0663	0.0397	0.0490	0.0544	0.0562	0.0457	0.0383	0.0499	0.0009	−0.0001	−0.0011	−0.0012	−0.0004	0.0003	0.0004	−0.0002
ALL	0.0551	0.0399	0.0455	0.0492	0.0484	0.0377	0.0335	0.0434	0.0514	0.0380	0.0448	0.0498	0.0487	0.0371	0.0329	0.0426	0.0037	0.0020	0.0007	−0.0006	−0.0003	0.0006	0.0006	0.0008

This table reports model accuracy in terms of options MAE(σ) within each moneyness-maturity category, with the estimations performed on the monthly data set. p − (c +) i refers to the put (call) options with strike equal to the ATM strike minus (plus) i USD. Only the central row refers to ATM options, all the others refer to OTM options; strikes are increasing. Sub-table (a) refers to TS09-SV1 and Sub-table (b) refers to SYSSV^S, both models expressed following the original characterisation of the parameters: observe that the darker the color of the cell (red), the worse the model performance. Sub-table (c) indicates the difference between both models: observe that the darker the color of the cell (blue), the better the performance of our model. Values of 0 indicate the lack of quoted options for this combination of contract and moneyness

Table 11 MAE(σ)—multiple harmonic pattern and original set-up

MAE(σ)	(a) TS09-SV1								(b) SYSSV^M								(c) Diff. TS09-SV1 − SYSSV^M							
	M2	M3	M4	M5	M6	M7	M8	ALL	M2	M3	M4	M5	M6	M7	M8	ALL	M2	M3	M4	M5	M6	M7	M8	ALL
p − 7.5	0.0798	0.0557	0.0502	0.0487	0.0424	0.0345	0.0328	0.0492	0.0623	0.0470	0.0473	0.0481	0.0416	0.0332	0.0321	0.0445	0.0174	0.0087	0.0029	0.0006	0.0007	0.0013	0.0007	0.0046
p − 7	0	0.0540	0.0504	0.0459	0.0425	0.0351	0.0337	0.0436	0	0.0468	0.0461	0.0455	0.0423	0.0334	0.0327	0.0411	0	0.0072	0.0043	0.0004	0.0002	0.0018	0.0010	0.0025
p − 6.5	0	0.0498	0.0486	0.0478	0.0420	0.0353	0.0327	0.0427	0	0.0440	0.0453	0.0473	0.0420	0.0341	0.0318	0.0407	0	0.0057	0.0033	0.0006	0.0000	0.0012	0.0009	0.0019
p − 6	0	0.0501	0.0483	0.0483	0.0447	0.0364	0.0327	0.0434	0	0.0442	0.0455	0.0480	0.0442	0.0351	0.0315	0.0414	0	0.0059	0.0029	0.0003	0.0005	0.0013	0.0011	0.0020
p − 5.5	0	0.0451	0.0478	0.0470	0.0440	0.0342	0.0320	0.0417	0	0.0397	0.0446	0.0467	0.0436	0.0328	0.0310	0.0397	0	0.0054	0.0032	0.0003	0.0003	0.0014	0.0011	0.0020
p − 5	0.0657	0.0445	0.0462	0.0465	0.0436	0.0340	0.0326	0.0447	0.0494	0.0393	0.0434	0.0460	0.0434	0.0328	0.0313	0.0408	0.0164	0.0052	0.0028	0.0006	0.0002	0.0012	0.0013	0.0039
p − 4.5	0.0937	0.0427	0.0451	0.0453	0.0457	0.0345	0.0317	0.0484	0.0785	0.0378	0.0422	0.0457	0.0457	0.0331	0.0306	0.0448	0.0153	0.0049	0.0028	−0.0004	0.0001	0.0014	0.0011	0.0036
p − 4	0.0532	0.0420	0.0444	0.0475	0.0438	0.0345	0.0316	0.0424	0.0437	0.0369	0.0413	0.0477	0.0440	0.0332	0.0303	0.0396	0.0095	0.0051	0.0030	−0.0001	0.0000	0.0013	0.0013	0.0028
p − 3.5	0.0463	0.0410	0.0445	0.0464	0.0454	0.0343	0.0319	0.0414	0.0396	0.0361	0.0420	0.0467	0.0452	0.0329	0.0308	0.0391	0.0067	0.0049	0.0026	−0.0002	−0.0002	0.0014	0.0011	0.0024
p − 3	0.0424	0.0398	0.0437	0.0473	0.0457	0.0353	0.0314	0.0408	0.0373	0.0354	0.0410	0.0470	0.0453	0.0339	0.0304	0.0386	0.0051	0.0045	0.0026	−0.0003	0.0004	0.0014	0.0010	0.0022
p − 2.5	0.0397	0.0389	0.0438	0.0478	0.0457	0.0357	0.0321	0.0405	0.0347	0.0344	0.0417	0.0474	0.0456	0.0345	0.0310	0.0385	0.0050	0.0044	0.0022	0.0002	0.0001	0.0013	0.0011	0.0020
p − 2	0	0.0372	0.0435	0.0472	0.0465	0.0337	0.0321	0.0400	0	0.0330	0.0410	0.0471	0.0464	0.0324	0.0309	0.0385	0	0.0042	0.0025	0.0003	0.0001	0.0013	0.0011	0.0016
p − 1.5	0.0388	0.0374	0.0444	0.0489	0.0494	0.0352	0.0327	0.0410	0.0333	0.0334	0.0421	0.0489	0.0492	0.0338	0.0316	0.0389	0.0056	0.0040	0.0023	0.0000	0.0002	0.0014	0.0010	0.0021
p − 1	0.0604	0.0367	0.0446	0.0491	0.0473	0.0375	0.0325	0.0440	0.0513	0.0329	0.0427	0.0490	0.0472	0.0364	0.0315	0.0416	0.0090	0.0039	0.0018	0.0002	0.0001	0.0011	0.0010	0.0024
p − 0.5	0.0378	0.0361	0.0443	0.0489	0.0480	0.0363	0.0318	0.0405	0.0322	0.0327	0.0427	0.0488	0.0476	0.0351	0.0310	0.0386	0.0057	0.0034	0.0016	0.0000	0.0004	0.0011	0.0008	0.0019
p − 0	0.0369	0.0354	0.0432	0.0472	0.0471	0.0351	0.0305	0.0393	0.0318	0.0320	0.0415	0.0469	0.0468	0.0341	0.0304	0.0377	0.0051	0.0033	0.0017	0.0003	0.0003	0.0010	0.0001	0.0017
c − 0	0.0371	0.0363	0.0445	0.0483	0.0471	0.0359	0.0324	0.0402	0.0317	0.0329	0.0431	0.0480	0.0468	0.0345	0.0317	0.0384	0.0054	0.0034	0.0014	0.0003	0.0003	0.0014	0.0007	0.0018
c − 0.5	0	0.0351	0.0430	0.0481	0.0476	0.0373	0.0315	0.0404	0	0.0319	0.0413	0.0480	0.0473	0.0361	0.0314	0.0393	0	0.0032	0.0016	0.0001	0.0003	0.0012	0.0001	0.0011
c − 1	0	0.0351	0.0434	0.0486	0.0481	0.0383	0.0317	0.0409	0	0.0321	0.0421	0.0485	0.0479	0.0372	0.0315	0.0399	0	0.0030	0.0013	0.0001	0.0002	0.0011	0.0002	0.0010
c − 1.5	0	0.0354	0.0434	0.0480	0.0481	0.0379	0.0323	0.0409	0	0.0328	0.0422	0.0479	0.0480	0.0370	0.0321	0.0400	0	0.0026	0.0012	0.0001	0.0002	0.0009	0.0002	0.0009
c − 2	0	0.0354	0.0442	0.0496	0.0490	0.0384	0.0325	0.0415	0	0.0331	0.0431	0.0495	0.0488	0.0375	0.0324	0.0408	0	0.0023	0.0011	0.0000	0.0002	0.0009	0.0001	0.0008
c − 2.5	0	0.0357	0.0442	0.0496	0.0501	0.0378	0.0337	0.0418	0	0.0337	0.0431	0.0495	0.0500	0.0372	0.0335	0.0412	0	0.0020	0.0010	0.0001	0.0001	0.0006	0.0002	0.0007
c − 3	0	0.0362	0.0447	0.0503	0.0499	0.0397	0.0342	0.0425	0	0.0344	0.0438	0.0503	0.0499	0.0390	0.0339	0.0419	0	0.0018	0.0009	0.0001	0.0000	0.0007	0.0003	0.0006
c − 3.5	0.0577	0.0368	0.0447	0.0502	0.0514	0.0389	0.0348	0.0449	0.0557	0.0352	0.0438	0.0501	0.0515	0.0387	0.0342	0.0442	0.0021	0.0015	0.0009	0.0001	−0.0001	0.0002	0.0005	0.0007
c − 4	0	0.0369	0.0451	0.0519	0.0519	0.0405	0.0350	0.0436	0	0.0356	0.0444	0.0517	0.0519	0.0402	0.0344	0.0430	0	0.0013	0.0008	0.0001	0.0000	0.0003	0.0006	0.0005
c − 4.5	0.0605	0.0371	0.0452	0.0521	0.0529	0.0412	0.0351	0.0463	0.0595	0.0360	0.0444	0.0519	0.0530	0.0404	0.0348	0.0457	0.0010	0.0011	0.0008	0.0002	−0.0001	0.0008	0.0003	0.0006
c − 5	0.0623	0.0375	0.0458	0.0513	0.0533	0.0411	0.0359	0.0467	0.0613	0.0365	0.0454	0.0513	0.0534	0.0409	0.0352	0.0463	0.0010	0.0009	0.0004	0.0000	−0.0002	0.0002	0.0007	0.0004
c − 5.5	0	0.0380	0.0463	0.0520	0.0536	0.0424	0.0374	0.0450	0	0.0374	0.0461	0.0518	0.0538	0.0417	0.0368	0.0446	0	0.0006	0.0002	0.0001	−0.0002	0.0007	0.0006	0.0004
c − 6	0.0567	0.0387	0.0466	0.0532	0.0559	0.0433	0.0372	0.0474	0.0562	0.0383	0.0463	0.0532	0.0559	0.0428	0.0367	0.0471	0.0006	0.0005	0.0003	0.0000	0.0000	0.0005	0.0004	0.0003
c − 6.5	0	0.0386	0.0472	0.0524	0.0556	0.0426	0.0371	0.0456	0	0.0383	0.0470	0.0523	0.0558	0.0419	0.0364	0.0453	0	0.0003	0.0002	0.0001	−0.0002	0.0007	0.0007	0.0003
c − 7	0	0.0396	0.0466	0.0545	0.0552	0.0438	0.0386	0.0463	0	0.0387	0.0465	0.0544	0.0554	0.0428	0.0381	0.0460	0	0.0002	0.0000	0.0002	−0.0002	0.0010	0.0006	0.0003
c − 7.5	0.0671	0.0396	0.0478	0.0532	0.0557	0.0459	0.0386	0.0497	0.0657	0.0395	0.0478	0.0531	0.0559	0.0452	0.0381	0.0493	0.0014	0.0001	0.0000	0.0002	−0.0002	0.0008	0.0006	0.0004
ALL	0.0551	0.0399	0.0455	0.0492	0.0484	0.0377	0.0335	0.0434	0.0485	0.0366	0.0438	0.0490	0.0483	0.0367	0.0328	0.0418	0.0066	0.0033	0.0017	0.0001	0.0001	0.0010	0.0007	0.0016

This table reports model accuracy in terms if options MAE(σ) within each moneyness-maturity category, with the estimations performed on the monthly data set. p − (c +) i refers to the put (call) options with strike equal to the ATM strike minus (plus) i USD. Only the central row refers to ATM options, all the others refer to OTM options; strikes are increasing. Sub-table (a) refers to TS09-SV1 and Sub-table (b) refers to SYSSV^M, both models expressed following the original characterisation of the parameters: observe that the darker the color of the cell (red), the worse the model performance. Sub-table (c) indicates the difference between both models: observe that the darker the color of the cell (blue), the better the performance of our model. Values of 0 indicate the lack of quoted options for this combination of contract and moneyness

Table 12 MAE(σ)—simple harmonic pattern and alternative set-up

MAE(σ)	(a) TS09-SV1								(b) SYSSV^S								(c) Diff. TS09-SV1 − SYSSV^S							
	M2	M3	M4	M5	M6	M7	M8	ALL	M2	M3	M4	M5	M6	M7	M8	ALL	M2	M3	M4	M5	M6	M7	M8	ALL
p – 7.5	0.0672	0.0450	0.0499	0.0515	0.0456	0.0337	0.0307	0.0462	0.0623	0.0470	0.0473	0.0481	0.0416	0.0332	0.0321	0.0445	0.0049	−0.0019	0.0026	0.0034	0.0040	0.0005	−0.0014	0.0017
p – 7	0	0.0430	0.0496	0.0481	0.0450	0.0334	0.0315	0.0418	0	0.0468	0.0461	0.0455	0.0423	0.0334	0.0327	0.0411	0	−0.0038	0.0034	0.0026	0.0027	0.0001	−0.0012	0.0006
p – 6.5	0	0.0412	0.0478	0.0495	0.0434	0.0341	0.0309	0.0411	0	0.0440	0.0453	0.0473	0.0420	0.0341	0.0318	0.0407	0	−0.0028	0.0025	0.0022	0.0014	0.0000	−0.0009	0.0004
p – 6	0	0.0415	0.0474	0.0493	0.0463	0.0350	0.0310	0.0417	0	0.0442	0.0455	0.0480	0.0442	0.0351	0.0315	0.0417	0	−0.0028	0.0019	0.0013	0.0021	−0.0001	−0.0005	0.0003
p – 5.5	0	0.0373	0.0467	0.0477	0.0451	0.0324	0.0306	0.0400	0	0.0397	0.0446	0.0467	0.0436	0.0328	0.0310	0.0397	0	−0.0024	0.0021	0.0010	0.0015	−0.0004	−0.0003	0.0002
p – 5	0.0594	0.0367	0.0451	0.0475	0.0445	0.0324	0.0310	0.0424	0.0494	0.0393	0.0434	0.0460	0.0434	0.0328	0.0313	0.0408	0.0101	−0.0026	0.0017	0.0015	0.0011	−0.0004	−0.0003	0.0016
p – 4.5	0.0593	0.0356	0.0438	0.0455	0.0463	0.0326	0.0308	0.0420	0.0785	0.0378	0.0422	0.0457	0.0457	0.0330	0.0306	0.0448	−0.0192	−0.0022	0.0016	−0.0002	0.0006	−0.0004	0.0001	−0.0028
p – 4	0.0576	0.0346	0.0429	0.0478	0.0442	0.0328	0.0310	0.0416	0.0437	0.0369	0.0413	0.0477	0.0440	0.0332	0.0303	0.0396	0.0139	−0.0023	0.0016	−0.0023	0.0002	−0.0004	0.0007	0.0020
p – 3.5	0.0580	0.0339	0.0433	0.0465	0.0459	0.0326	0.0315	0.0417	0.0396	0.0361	0.0420	0.0467	0.0452	0.0329	0.0308	0.0391	0.0184	−0.0023	0.0013	−0.0002	0.0007	−0.0004	−0.0007	0.0026
p – 3	0.0577	0.0337	0.0422	0.0473	0.0458	0.0336	0.0312	0.0416	0.0373	0.0354	0.0410	0.0470	0.0453	0.0339	0.0304	0.0386	0.0204	−0.0017	0.0012	0.0002	0.0005	−0.0003	0.0008	0.0030
p – 2.5	0.0593	0.0328	0.0426	0.0479	0.0456	0.0342	0.0318	0.0420	0.0347	0.0344	0.0417	0.0474	0.0456	0.0345	0.0310	0.0385	0.0245	−0.0017	0.0010	0.0004	0.0000	−0.0003	0.0008	0.0035
p – 2	0	0.0319	0.0422	0.0471	0.0466	0.0322	0.0321	0.0387	0.0330	0.0330	0.0410	0.0471	0.0464	0.0324	0.0309	0.0385	0	−0.0011	0.0012	0.0000	0.0002	−0.0002	0.0012	0.0002
p – 1.5	0.0625	0.0324	0.0432	0.0485	0.0491	0.0337	0.0327	0.0431	0.0333	0.0334	0.0421	0.0489	0.0492	0.0338	0.0316	0.0389	0.0292	−0.0010	0.0011	−0.0005	−0.0002	−0.0001	0.0011	0.0042
p – 1	0.0506	0.0318	0.0436	0.0489	0.0471	0.0363	0.0335	0.0417	0.0513	0.0329	0.0427	0.0490	0.0472	0.0364	0.0315	0.0416	−0.0007	−0.0011	0.0009	0.0000	−0.0001	−0.0001	0.002	0.0001
p – 0.5	0.0660	0.0323	0.0435	0.0487	0.0481	0.0351	0.0327	0.0438	0.0322	0.0327	0.0427	0.0488	0.0476	0.0351	0.0310	0.0386	0.0338	−0.0004	0.0008	−0.0002	−0.0004	−0.0001	0.0017	0.0052
p – 0	0.0662	0.0322	0.0423	0.0471	0.0472	0.0341	0.0320	0.0430	0.0318	0.0320	0.0415	0.0469	0.0468	0.0341	0.0304	0.0377	0.0344	0.0002	0.0008	0.0002	0.0004	0.0000	0.0016	0.0054
c – 0	0.0675	0.0327	0.0438	0.0484	0.0473	0.0346	0.0332	0.0439	0.0317	0.0329	0.0431	0.0480	0.0468	0.0345	0.0317	0.0384	0.0358	−0.0002	0.0007	0.0003	0.0005	0.0001	0.0015	0.0055
c – 0.5	0	0.0324	0.0421	0.0478	0.0478	0.0362	0.0331	0.0399	0	0.0319	0.0413	0.0480	0.0473	0.0361	0.0314	0.0393	0	0.0006	0.0008	−0.0002	0.0005	0.0002	0.0017	0.0006
c – 1	0	0.0332	0.0428	0.0484	0.0484	0.0372	0.0334	0.0406	0	0.0321	0.0421	0.0485	0.0479	0.0372	0.0315	0.0399	0	0.0011	0.0007	−0.0001	0.0005	0.0000	0.0018	0.0007
c – 1.5	0	0.0343	0.0429	0.0480	0.0483	0.0371	0.0338	0.0407	0	0.0328	0.0422	0.0479	0.0480	0.0370	0.0321	0.0400	0	0.0014	0.0007	0.0000	0.0003	0.0001	0.0017	0.0007
c – 2	0	0.0348	0.0438	0.0492	0.0494	0.0378	0.0340	0.0415	0	0.0331	0.0431	0.0495	0.0488	0.0375	0.0324	0.0408	0	0.0017	0.0006	−0.0003	0.0006	0.0002	0.0016	0.0007
c – 2.5	0	0.0356	0.0437	0.0494	0.0506	0.0374	0.0351	0.0420	0	0.0337	0.0431	0.0495	0.0500	0.0372	0.0335	0.0412	0	0.0019	0.0006	−0.0001	0.0006	0.0002	0.0016	0.0008
c – 3	0	0.0366	0.0443	0.0501	0.0504	0.0393	0.0357	0.0427	0	0.0344	0.0438	0.0503	0.0499	0.0390	0.0339	0.0419	0	0.0021	0.0006	−0.0002	0.0006	0.0002	0.0018	0.0009
c – 3.5	0.0557	0.0374	0.0444	0.0502	0.0519	0.0389	0.0358	0.0456	0.0557	0.0352	0.0438	0.0501	0.0515	0.0387	0.0342	0.0442	0.0047	0.0022	0.0006	0.0002	0.0004	0.0002	0.0015	0.0014
c – 4	0	0.0379	0.0448	0.0517	0.0525	0.0405	0.0366	0.0440	0	0.0356	0.0444	0.0517	0.0519	0.0402	0.0344	0.0430	0	0.0023	0.0004	0.0000	0.0006	0.0003	0.0022	0.0010
c – 4.5	0.0612	0.0382	0.0448	0.0521	0.0534	0.0408	0.0364	0.0467	0.0595	0.036	0.0444	0.0519	0.0530	0.0404	0.0348	0.0457	0.0017	0.0022	0.0003	0.0002	0.0004	0.0004	0.0016	0.0010
c – 5	0.0610	0.0391	0.0456	0.0511	0.0541	0.0412	0.0372	0.0470	0.0613	0.0365	0.0454	0.0513	0.0534	0.0409	0.0352	0.0463	−0.0004	0.0026	0.0002	−0.0002	0.0006	0.0003	0.002	0.0008
c – 5.5	0	0.0399	0.0463	0.0520	0.0543	0.0422	0.0390	0.0456	0	0.0374	0.0461	0.0518	0.0538	0.0417	0.0368	0.0446	0	0.0025	0.0001	0.0001	0.0006	0.0005	0.0022	0.0010
c – 6	0.0618	0.0402	0.0464	0.0529	0.0561	0.0432	0.0384	0.0485	0.0562	0.0383	0.0463	0.0532	0.0559	0.0428	0.0367	0.0471	0.0057	0.0019	0.0001	−0.0003	0.0002	0.0004	0.0017	0.0014
c – 6.5	0	0.0405	0.0470	0.0522	0.0563	0.0424	0.0385	0.0462	0	0.0383	0.0470	0.0523	0.0558	0.0419	0.0364	0.0453	0	0.0022	0.0000	−0.0001	0.0005	0.0005	0.0021	0.0009
c – 7	0	0.0404	0.0463	0.0546	0.0560	0.0433	0.0399	0.0467	0	0.0387	0.0465	0.0544	0.0554	0.0428	0.0380	0.0460	0	0.0016	−0.0002	0.0002	0.0006	0.0005	0.0020	0.0008
c – 7.5	0.0626	0.0410	0.0475	0.0534	0.0565	0.0455	0.0394	0.0494	0.0657	0.0395	0.0478	0.0531	0.0559	0.0452	0.0381	0.0493	−0.0032	0.0015	−0.0003	0.0003	0.0006	0.0004	0.0013	0.0001
ALL	0.0611	0.0366	0.0448	0.0494	0.0490	0.0367	0.0339	0.0433	0.0485	0.0366	0.0438	0.0490	0.0483	0.0367	0.0328	0.0418	−0.0126	−0.0001	0.0010	0.0004	0.0007	0.0001	0.0011	0.0015

This table reports model accuracy in terms if options MAE(σ) within each moneyness-maturity category, with the estimations performed on the monthly data set. p − (c +) i refers to the put (call) options with strike equal to the ATM strike minus (plus) i USD. Only the central row refers to ATM options, all the others refer to OTM options; strikes are increasing. Sub-table (a) refers to TS09-SV1 and Sub-table (b) refers to SYSSV^S, both models expressed following the original characterisation of the parameters: observe that the darker the color of the cell (red), the worse the model performance. Sub-table (c) indicates the difference between both models: observe that the darker the color of the cell (blue), the better the performance of our model. Values of 0 indicate the lack of quoted options for this combination of contract and moneyness

Table 13 MAE(σ)—multiple harmonic pattern and alternative set-up

MAE(σ)	(a) TS09-SV1								(b) SYSSV^M								(c) Diff. TS09-SV1 − SYSSV^M							
	M2	M3	M4	M5	M6	M7	M8	ALL	M2	M3	M4	M5	M6	M7	M8	ALL	M2	M3	M4	M5	M6	M7	M8	ALL
p − 7.5	0.0672	0.0450	0.0499	0.0515	0.0456	0.0337	0.0307	0.0462	0.0609	0.0453	0.0479	0.0489	0.0426	0.0334	0.0308	0.0443	0.0063	−0.0002	0.0020	0.0026	0.0030	0.0003	0.0000	0.0020
p − 7	0	0.0430	0.0496	0.0481	0.0450	0.0334	0.0315	0.0418	0	0.0433	0.0476	0.0460	0.0427	0.0335	0.0307	0.0406	0	−0.0003	0.0020	0.0021	0.0023	−0.0001	0.0007	0.0011
p − 6.5	0	0.0412	0.0478	0.0495	0.0434	0.0341	0.0309	0.0411	0	0.0419	0.0467	0.0481	0.0423	0.0342	0.0306	0.0406	0	−0.0006	0.0011	0.0014	0.0011	−0.0002	0.0003	0.0005
p − 6	0	0.0415	0.0474	0.0493	0.0463	0.0350	0.0310	0.0417	0	0.0426	0.0470	0.0486	0.0449	0.0353	0.0300	0.0414	0	−0.0012	0.0004	0.0007	0.0014	−0.0003	0.0010	0.0003
p − 5.5	0	0.0373	0.0467	0.0477	0.0451	0.0324	0.0306	0.0400	0	0.0384	0.0464	0.0476	0.0441	0.0329	0.0296	0.0398	0	−0.0011	0.0004	0.0001	0.0011	−0.0005	0.0010	0.0002
p − 5	0.0594	0.0367	0.0451	0.0475	0.0445	0.0324	0.0310	0.0424	0.0490	0.0378	0.0451	0.0467	0.0438	0.0329	0.0298	0.0407	0.0104	−0.0012	0.0000	0.0008	0.0007	−0.0005	0.0012	0.0016
p − 4.5	0.0593	0.0356	0.0438	0.0455	0.0463	0.0326	0.0310	0.0420	0.0580	0.0365	0.0439	0.0459	0.0459	0.0332	0.0298	0.0419	0.0012	−0.0010	−0.0001	−0.0004	0.0004	−0.0006	0.0010	0.0001
p − 4	0.0576	0.0346	0.0429	0.0478	0.0442	0.0328	0.0310	0.0416	0.0441	0.0355	0.0441	0.0482	0.0441	0.0333	0.0292	0.0396	0.0135	−0.0009	−0.0002	−0.0004	0.0001	−0.0005	0.0018	0.0019
p − 3.5	0.0580	0.0339	0.0433	0.0465	0.0459	0.0326	0.0315	0.0417	0.0413	0.0348	0.0436	0.0470	0.0455	0.0331	0.0300	0.0393	0.0167	−0.0009	−0.0004	−0.0005	0.0004	−0.0006	0.0015	0.0023
p − 3	0.0577	0.0337	0.0422	0.0473	0.0458	0.0336	0.0312	0.0416	0.0385	0.0341	0.0428	0.0477	0.0458	0.0341	0.0298	0.0390	0.0192	−0.0004	−0.0006	−0.0005	0.0001	−0.0005	0.0013	0.0027
p − 2.5	0.0593	0.0328	0.0426	0.0479	0.0456	0.0342	0.0318	0.0420	0.0366	0.0331	0.0428	0.0481	0.0460	0.0347	0.0305	0.0389	0.0227	−0.0004	−0.0007	−0.0002	−0.0004	−0.0005	0.0013	0.0031
p − 2	0	0.0319	0.0422	0.0471	0.0466	0.0322	0.0321	0.0387	0	0.0318	0.0428	0.0476	0.0467	0.0327	0.0305	0.0387	0	0.0001	−0.0006	−0.0005	−0.0002	−0.0005	0.0016	0.0000
p − 1.5	0.0625	0.0324	0.0432	0.0485	0.0491	0.0337	0.0327	0.0431	0.0332	0.0323	0.0439	0.0495	0.0497	0.0342	0.0311	0.0391	0.0292	0.0001	−0.0007	−0.0010	−0.0006	−0.0005	0.0016	0.0040
p − 1	0.0506	0.0318	0.0436	0.0489	0.0471	0.0363	0.0335	0.0417	0.0181	0.0315	0.0443	0.0496	0.0476	0.0365	0.0313	0.0370	0.0325	0.0003	−0.0007	−0.0007	−0.0005	−0.0003	0.0022	0.0047
p − 0.5	0.0660	0.0323	0.0435	0.0487	0.0481	0.0351	0.0327	0.0438	0.0319	0.0315	0.0443	0.0492	0.0481	0.0354	0.0309	0.0388	0.0342	0.0008	−0.0007	−0.0005	−0.0001	−0.0003	0.0010	0.0050
p − 0	0.0662	0.0322	0.0423	0.0471	0.0472	0.0341	0.0320	0.0430	0.0316	0.0309	0.0430	0.0475	0.0473	0.0344	0.0310	0.0379	0.0346	0.0014	−0.0007	−0.0004	−0.0001	−0.0003	0.0010	0.0051
c − 0	0.0675	0.0327	0.0438	0.0484	0.0473	0.0346	0.0332	0.0439	0.0323	0.0316	0.0445	0.0486	0.0472	0.0349	0.0317	0.0387	0.0353	0.0011	−0.0007	−0.0002	0.0001	−0.0004	0.0014	0.0052
c − 0.5	0	0.0324	0.0421	0.0478	0.0478	0.0362	0.0331	0.0399	0	0.0309	0.0428	0.0485	0.0478	0.0367	0.0319	0.0398	0	0.0016	−0.0007	−0.0007	0.0000	−0.0004	0.0012	0.0002
c − 1	0	0.0332	0.0428	0.0484	0.0484	0.0372	0.0334	0.0406	0	0.0315	0.0434	0.0490	0.0483	0.0376	0.0319	0.0403	0	0.0017	−0.0006	−0.0006	0.0001	−0.0004	0.0015	0.0003
c − 1.5	0	0.0343	0.0429	0.0480	0.0483	0.0371	0.0338	0.0407	0	0.0323	0.0436	0.0484	0.0484	0.0374	0.0325	0.0404	0	0.0019	−0.0007	−0.0005	−0.0001	−0.0003	0.0014	0.0003
c − 2	0	0.0348	0.0438	0.0492	0.0494	0.0378	0.0340	0.0415	0	0.0326	0.0444	0.0501	0.0492	0.0381	0.0327	0.0412	0	0.0022	−0.0007	−0.0008	0.0002	−0.0003	0.0014	0.0003
c − 2.5	0	0.0356	0.0437	0.0494	0.0506	0.0374	0.0351	0.0420	0	0.0332	0.0443	0.0502	0.0502	0.0376	0.0339	0.0415	0	0.0024	−0.0006	−0.0007	−0.0007	−0.0002	0.0012	0.0004
c − 3	0	0.0366	0.0443	0.0501	0.0504	0.0393	0.0357	0.0427	0	0.0343	0.0451	0.0501	0.0501	0.0395	0.0341	0.0423	0	0.0023	−0.0007	−0.0007	0.0004	−0.0002	0.0016	0.0004
c − 3.5	0.0604	0.0374	0.0444	0.0502	0.0519	0.0389	0.0358	0.0456	0.0408	0.0353	0.0451	0.0506	0.0515	0.0390	0.0344	0.0424	0.0195	0.0021	−0.0008	−0.0004	0.0004	−0.0001	0.0014	0.0032
c − 4	0	0.0379	0.0448	0.0517	0.0525	0.0405	0.0366	0.0440	0	0.0360	0.0456	0.0525	0.0520	0.0407	0.0347	0.0436	0	0.0020	−0.0008	−0.0007	0.0005	−0.0002	0.0019	0.0004
c − 4.5	0.0612	0.0382	0.0448	0.0521	0.0534	0.0408	0.0364	0.0467	0.0472	0.0364	0.0456	0.0525	0.0530	0.0412	0.0352	0.0445	0.0140	0.0018	−0.0008	−0.0004	0.0004	−0.0004	0.0012	0.0023
c − 5	0.0610	0.0391	0.0456	0.0511	0.0541	0.0412	0.0372	0.0470	0.0492	0.0374	0.0466	0.0519	0.0533	0.0414	0.0355	0.0450	0.0117	0.0018	−0.0010	−0.0008	0.0008	−0.0002	0.0017	0.0020
c − 5.5	0	0.0399	0.0463	0.0520	0.0543	0.0422	0.0390	0.0456	0	0.0383	0.0473	0.0524	0.0536	0.0426	0.0371	0.0452	0	0.0016	−0.0010	−0.0005	0.0007	−0.0004	0.0019	0.0004
c − 6	0.0618	0.0402	0.0464	0.0529	0.0561	0.0432	0.0384	0.0485	0.0507	0.0390	0.0476	0.0538	0.0560	0.0435	0.0372	0.0468	0.0111	0.0013	−0.0012	−0.0009	0.0001	−0.0003	0.0013	0.0016
c − 6.5	0	0.0405	0.0470	0.0522	0.0563	0.0424	0.0385	0.0462	0	0.0394	0.0484	0.0529	0.0556	0.0428	0.0367	0.0460	0	0.0011	−0.0014	−0.0006	0.0007	−0.0003	0.0018	0.0002
c − 7	0	0.0404	0.0463	0.0546	0.0560	0.0433	0.0399	0.0467	0	0.0398	0.0477	0.0551	0.0553	0.0439	0.0384	0.0467	0	0.0006	−0.0015	−0.0005	0.0007	−0.0005	0.0016	0.0001
c − 7.5	0.0626	0.0410	0.0475	0.0534	0.0565	0.0455	0.0394	0.0494	0.0558	0.0405	0.0490	0.0536	0.0558	0.0461	0.0383	0.0484	0.0067	0.0005	−0.0015	−0.0002	0.0007	−0.0005	0.0011	0.0010
ALL	0.0611	0.0366	0.0448	0.0494	0.0490	0.0367	0.0339	0.0433	0.0423	0.0359	0.0452	0.0496	0.0486	0.0371	0.0326	0.0416	0.0188	0.0006	−0.0004	−0.0002	0.0005	−0.0003	0.0013	0.0017

This table reports model accuracy in terms of options MAE(σ) within each moneyness-maturity category, with the estimations performed on the monthly data set. p − (c +) i refers to the put (call) options with strike equal to the ATM strike minus (plus) i USD. Only the central row refers to ATM options, all the others refer to OTM options; strikes are increasing. Sub-table (a) refers to TS09-SV1 and Sub-table (b) refers to SYSSV^M, both models expressed following the original characterisation of the parameters: observe that the darker the color of the cell (red), the worse the model performance. Sub-table (c) indicates the difference between both models: observe that the darker the color of the cell (blue), the better the performance of our model. Values of 0 indicate the lack of quoted options for this combination of contract and moneyness

Table 14 MAE(σ)—simple harmonic patterns

MAE(σ)	(a) SYSSV^S								(b) ST21								(c) Diff. ST21 − SYSSV^S							
	M2	M3	M4	M5	M6	M7	M8	ALL	M2	M3	M4	M5	M6	M7	M8	ALL	M2	M3	M4	M5	M6	M7	M8	ALL
p − 7.5	0.0623	0.0470	0.0473	0.0481	0.0416	0.0332	0.0321	0.0445	0.0387	0.0574	0.0529	0.0507	0.0433	0.0326	0.0320	0.0518	0.0313	0.0104	0.0056	0.0026	0.0016	−0.0006	−0.0002	0.0073
p − 7	0	0.0468	0.0455	0.0461	0.0420	0.0334	0.0327	0.0411	0	0.0544	0.0527	0.0472	0.0430	0.0331	0.0324	0.0438	0	0.0076	0.0066	0.0016	0.0008	−0.0003	−0.0003	0.0027
p − 6.5	0	0.0440	0.0453	0.0473	0.0420	0.0341	0.0318	0.0407	0	0.0503	0.0507	0.0489	0.0422	0.0338	0.0316	0.0429	0	0.0063	0.0054	0.0016	0.0003	−0.0003	−0.0002	0.0022
p − 6	0	0.0442	0.0455	0.0480	0.0442	0.0351	0.0315	0.0414	0	0.0506	0.0501	0.0487	0.0450	0.0351	0.0317	0.0435	0	0.0064	0.0046	0.0007	0.0007	0.0000	0.0002	0.0021
p − 5.5	0	0.0397	0.0446	0.0467	0.0436	0.0328	0.0310	0.0397	0	0.0455	0.0492	0.0473	0.0441	0.0328	0.0310	0.0417	0	0.0058	0.0046	0.0006	0.0005	0.0001	0.0000	0.0019
p − 5	0.0494	0.0393	0.0434	0.0460	0.0434	0.0328	0.0313	0.0408	0.0574	0.0447	0.0473	0.0452	0.0437	0.0328	0.0317	0.0436	0.0081	0.0054	0.0040	0.0011	0.0004	0.0000	0.0005	0.0028
p − 4.5	0.0785	0.0378	0.0422	0.0457	0.0457	0.0330	0.0306	0.0448	0.0947	0.0430	0.0459	0.0452	0.0455	0.0332	0.0314	0.0484	0.0163	0.0052	0.0037	−0.0005	−0.0002	0.0001	0.0007	0.0036
p − 4	0.0437	0.0369	0.0413	0.0477	0.0440	0.0332	0.0303	0.0396	0.0491	0.0423	0.0450	0.0476	0.0435	0.0329	0.0310	0.0416	0.0054	0.0053	0.0037	−0.0001	−0.0004	−0.0003	0.0007	0.0020
p − 3.5	0.0396	0.0361	0.0420	0.0467	0.0452	0.0329	0.0308	0.0391	0.0444	0.0411	0.0451	0.0462	0.0450	0.0328	0.0316	0.0409	0.0048	0.0050	0.0032	−0.0005	−0.0002	−0.0001	0.0008	0.0018
p − 3	0.0373	0.0354	0.0410	0.0470	0.0453	0.0339	0.0304	0.0386	0.0423	0.0399	0.0442	0.0471	0.0454	0.0336	0.0312	0.0405	0.0050	0.0046	0.0032	0.0001	0.0002	−0.0003	0.0008	0.0019
p − 2.5	0.0347	0.0344	0.0417	0.0474	0.0456	0.0345	0.0310	0.0385	0.0398	0.0389	0.0444	0.0477	0.0453	0.0340	0.0316	0.0402	0.0050	0.0044	0.0027	0.0003	−0.0003	−0.0005	0.0006	0.0017
p − 2	0	0.0330	0.0410	0.0471	0.0464	0.0324	0.0309	0.0385	0	0.0373	0.0439	0.0469	0.0460	0.0326	0.0319	0.0398	0	0.0043	0.0029	−0.0002	−0.0004	0.0002	0.0010	0.0013
p − 1.5	0.0333	0.0334	0.0421	0.0489	0.0492	0.0338	0.0316	0.0389	0.0383	0.0375	0.0449	0.0489	0.0468	0.0336	0.0327	0.0406	0.0050	0.0041	0.0027	−0.0004	−0.0003	−0.0002	0.0010	0.0017
p − 1	0.0513	0.0329	0.0427	0.0490	0.0472	0.0364	0.0315	0.0416	0.0603	0.0369	0.0449	0.0489	0.0468	0.0364	0.0327	0.0438	0.0090	0.0040	0.0021	0.0000	0.0000	−0.0001	0.0012	0.0023
p − 0.5	0.0322	0.0327	0.0427	0.0488	0.0476	0.0351	0.0310	0.0386	0.0367	0.0364	0.0447	0.0484	0.0476	0.0353	0.0321	0.0402	0.0045	0.0037	0.0020	−0.0005	0.0000	0.0002	0.0011	0.0016
p − 0	0.0318	0.0320	0.0415	0.0469	0.0468	0.0341	0.0304	0.0377	0.0361	0.0356	0.0436	0.0470	0.0466	0.0341	0.0308	0.0391	0.0043	0.0036	0.0021	0.0001	−0.0002	−0.0001	0.0004	0.0015
c − 0	0.0317	0.0329	0.0431	0.0480	0.0468	0.0345	0.0317	0.0384	0.0360	0.0367	0.0449	0.0483	0.0466	0.0350	0.0324	0.0400	0.0043	0.0038	0.0018	0.0002	−0.0002	0.0005	0.0006	0.0016
c − 0.5	0	0.0319	0.0413	0.0480	0.0473	0.0361	0.0314	0.0393	0	0.0356	0.0435	0.0477	0.0472	0.0354	0.0318	0.0402	0	0.0037	0.0021	−0.0003	−0.0001	−0.0006	0.0005	0.0009
c − 1	0	0.0321	0.0421	0.0485	0.0479	0.0372	0.0315	0.0399	0	0.0358	0.0440	0.0482	0.0477	0.0369	0.0321	0.0408	0	0.0036	0.0019	−0.0003	−0.0002	−0.0003	0.0006	0.0009
c − 1.5	0	0.0328	0.0422	0.0479	0.0480	0.0370	0.0321	0.0400	0	0.0362	0.0439	0.0477	0.0477	0.0363	0.0327	0.0408	0	0.0033	0.0017	−0.0002	−0.0003	−0.0007	0.0006	0.0007
c − 2	0	0.0331	0.0431	0.0495	0.0488	0.0375	0.0324	0.0408	0	0.0363	0.0447	0.0491	0.0485	0.0369	0.0332	0.0415	0	0.0032	0.0016	−0.0005	−0.0003	−0.0006	0.0007	0.0007
c − 2.5	0	0.0337	0.0431	0.0495	0.0500	0.0372	0.0335	0.0412	0	0.0367	0.0448	0.0492	0.0496	0.0364	0.0340	0.0418	0	0.0031	0.0017	−0.0004	−0.0005	−0.0008	0.0005	0.0006
c − 3	0	0.0344	0.0438	0.0503	0.0499	0.0390	0.0339	0.0419	0	0.0374	0.0453	0.0499	0.0494	0.0383	0.0348	0.0425	0	0.0029	0.0016	−0.0004	−0.0005	−0.0007	0.0009	0.0006
c − 3.5	0.0557	0.0352	0.0438	0.0501	0.0515	0.0387	0.0342	0.0442	0.0594	0.0380	0.0455	0.0499	0.0507	0.0377	0.0349	0.0452	0.0038	0.0028	0.0016	−0.0002	−0.0008	−0.0010	0.0007	0.0010
c − 4	0	0.0356	0.0444	0.0517	0.0519	0.0402	0.0344	0.0430	0	0.0383	0.0459	0.0515	0.0513	0.0393	0.0355	0.0436	0	0.0027	0.0015	−0.0002	−0.0006	−0.0009	0.0011	0.0006
c − 4.5	0.0595	0.0360	0.0444	0.0519	0.0530	0.0404	0.0348	0.0457	0.0631	0.0386	0.0462	0.0518	0.0523	0.0397	0.0355	0.0467	0.0035	0.0026	0.0017	−0.0001	−0.0006	−0.0008	0.0007	0.0010
c − 5	0.0613	0.0365	0.0454	0.0513	0.0534	0.0409	0.0352	0.0463	0.0667	0.0391	0.0466	0.0508	0.0527	0.0397	0.0363	0.0474	0.0053	0.0026	0.0012	−0.0005	−0.0008	−0.0012	0.0012	0.0011
c − 5.5	0	0.0374	0.0461	0.0518	0.0538	0.0417	0.0368	0.0446	0	0.0397	0.0471	0.0516	0.0529	0.0406	0.0379	0.0450	0	0.0024	0.0009	−0.0002	−0.0009	−0.0011	0.0011	0.0004
c − 6	0.0562	0.0383	0.0463	0.0532	0.0559	0.0428	0.0367	0.0471	0.0625	0.0406	0.0475	0.0526	0.0550	0.0416	0.0376	0.0482	0.0064	0.0024	0.0011	−0.0006	−0.0009	−0.0013	0.0008	0.0011
c − 6.5	0	0.0383	0.0470	0.0523	0.0558	0.0419	0.0364	0.0453	0	0.0406	0.0477	0.0517	0.0548	0.0406	0.0376	0.0455	0	0.0024	0.0007	−0.0006	−0.0010	−0.0013	0.0012	0.0002
c − 7	0	0.0387	0.0465	0.0544	0.0554	0.0428	0.0380	0.0460	0	0.0410	0.0472	0.0541	0.0544	0.0417	0.0388	0.0462	0	0.0023	0.0007	−0.0004	−0.0010	−0.0012	0.0009	0.0002
c − 7.5	0.0657	0.0395	0.0478	0.0531	0.0559	0.0452	0.0381	0.0493	0.0757	0.0421	0.0483	0.0527	0.0548	0.0438	0.0385	0.0508	0.0100	0.0026	0.0006	−0.0003	−0.0011	−0.0014	0.0004	0.0015
ALL	0.0485	0.0366	0.0438	0.0490	0.0483	0.0367	0.0328	0.0418	0.0562	0.0408	0.0463	0.0491	0.0481	0.0362	0.0335	0.0434	0.0078	0.0041	0.0025	0.0001	−0.0002	−0.0005	0.0006	0.0017

This table reports model accuracy in terms of options MAE(σ) within each moneyness-maturity category, with the estimations performed on the monthly data set. p − (c +) i refers to the put (call) options with strike equal to the ATM strike minus (plus) i USD. Only the central row refers to ATM options, all the others refer to OTM options; strikes are increasing. Sub-table (a) refers to our model SYSSV^S and Sub-table (b) refers to ST21, our model expressed following the alternative characterisation of the parameters (ST21) implicitly follows also it), both models following the same simple harmonic function: observe that the darker the color of the cell (red), the worse the model performance. Sub-table (c) indicates the difference between both models: observe that the darker the color of the cell (blue), the better the performance of our model. Values of 0 indicate the lack of quoted options for this combination of contract and moneyness

We had initially expected Hes93 and more clearly Mer76 to underperform compared to our model and benchmark, given that jump models' parameters are quite unstable.

5 Conclusions and further research

Volatility in many commodity markets follows a pronounced seasonal pattern while also fluctuating stochastically. In this paper, we extend the stochastic volatility model of TS09-SV1 to allow volatility to vary with the seasonal cycle. We have developed a model that enables deriving quasi-closed-form solutions for pricing options on futures prices. We empirically study its performance in pricing HH natural gas standard European options. We estimate our model using a cross-section of options prices considering a series of 10 years of futures contracts. Results show that the SSV model we suggest increases the accuracy of pricing options on HH natural gas. When our models follows an original set-up, accuracy increases especially for shorter maturity contracts and deeper OTM options. We also propose an alternative set-up, whereby we obtain better pricing performance for shorter maturity contracts and closer to the ATM options. An additional benefit of this alternative set-up consists of improving the speed of calculation.

We conclude the paper by outlining areas for future research. Many commodity assets exhibit jumps not only in prices but also in volatility, especially the natural gas. We identify that the jump model in Bat96 slightly outperforms our model and its benchmark; we can leverage this finding to study the inclusion of jumps in a future line of research. We also consider modeling the jump intensity according to a seasonal function. Another research field of interest are calendar spread options which are also common in energy markets, and their pricing requires to know the expression followed by the joint CF for the two futures involved.

A Appendix for proofs

A.1 Proof of Proposition 1

We find the expressions followed by the terms $A(\tau)$ and $B(\tau)$ similarly to Duffie et al. (2000) and Collin-Dufresne and Goldstein (2002). The proof consists of showing that the process $\psi(t) \equiv \psi(iu; t, T_{Opt}, T)$ is a martingale under $\mathbb{Q}$. To this end, we conjecture that $\psi(iu; t, T_{Opt}, T)$ is of the form in Eq. (2.21). From applying Itô's Lemma for jump diffusion processes to $\psi(t)$, we obtain the following partial integro-differential equation (PIDE)

$$\frac{d\psi(t)}{\psi(t)} = -\left(\frac{\partial A(T_{Opt} - t)}{\partial(T_{Opt} - t)} + \frac{\partial B(T_{Opt} - t)}{\partial(T_{Opt} - t)} v_t \right) dt + B(T_{Opt} - t)dv_t + iu \frac{dF(t, T)}{F(t, T)}$$

$$+ \frac{1}{2} B^2(T_{Opt} - t)dv_t^2$$

$$-\frac{1}{2}(u^2 + iu)\left(\frac{dF(t,T)}{F(t,T)}\right)^2 + iuB(T_{Opt} - t)dv_t\frac{dF(t,T)}{F(t,T)}. \tag{A.1}$$

For $\psi(t)$ to be a martingale and with $\tau \equiv T_{Opt} - t$, it must hold that

$$\frac{1}{dt}E_t^{\mathbb{Q}}\left[\frac{d\psi(t)}{\psi(t)}\right] = \left(-\frac{\partial A(\tau)}{\partial\tau} + B(\tau)\kappa\,\theta_t\right) + \left(-\frac{\partial B(\tau)}{\partial\tau} + b_0 + b_1B(\tau) + b_2B^2(\tau)\right)v_t = 0. \tag{A.2}$$

Subject to the initial condition $B(0) = 0$ and conditional to the original parameters set-up, we have that

$$b_0 = -\frac{1}{2}(u^2 + iu)\left(\sigma_S^2 + \sigma_Y^2(t,T) + 2\rho_{Sy}\sigma_S\sigma_Y(t,T)\right), \tag{A.3}$$

$$b_1 = -\kappa + iu\sigma_v\left(\rho_{Sv}\sigma_S + \rho_{yv}\sigma_Y(t,T)\right), \tag{A.4}$$

and conditional to our alternative set-up (as defined in Sect. 2.1.2), we have that

$$b_0 = -\frac{1}{2}(u^2 + iu)\sigma_F^2(t,T), \tag{A.5}$$

$$b_1 = -\kappa + iu\sigma_v\rho_{Fv}\sigma_F(t,T), \tag{A.6}$$

and the constant term b_2 being unconditional to the set-up

$$b_2 = \frac{\sigma_v^2}{2}. \tag{A.7}$$

Since Eq. (A.2) holds for all t, $f(t,T)$ and v_t then the terms in each parentheses must vanish, reducing the problem to solving two much simpler ODEs

$$\frac{\partial A(\tau)}{\partial\tau} = B(\tau)\kappa\,\theta_t, \tag{A.8}$$

$$\frac{\partial B(\tau)}{\partial\tau} = b_0 + b_1B(\tau) + b_2B^2(\tau). \tag{A.9}$$

Hence, $\psi(t)$ is a martingale provided that $A(\tau)$ and $B(\tau)$ satisfy (A.8) and (A.9), respectively. The expression followed by $B(\tau)$ can be found in Appendix B.1. Depending on the functional form followed by θ_t, the solution to $A(\tau)$ can be found in Appendix A.2 (single sinusoidal pattern) or A.3 (mixed sinusoidal pattern).

A.2 Proof of Proposition 2

With $B(\tau)$ as in Eq. (2.25) and θ_t following the single sinusoidal pattern defined in expression (2.5), Eq. (2.22) becomes[16]

$$\begin{aligned}\frac{\partial A(\tau)}{\partial\tau} &= B(\tau)\kappa\left(a^\theta + b^\theta\cos\left(2\pi(T_{Opt} - \tau - t_0)\right)\right)\\ &= \frac{2\kappa\gamma}{\sigma_v^2}\left(\beta + \mu z + z\frac{g'(z)}{g(z)}\right)\left(a^\theta + b^\theta\cos\left(2\pi(T_{Opt} - \tau - t_0)\right)\right)\\ &= m\left(A_1'(\tau) + A_2'(\tau) + A_3'(\tau) + A_4'(\tau)\right),\end{aligned} \tag{A.10}$$

---

[16] Given that $\tau \equiv T_{Opt} - t$, we use the equality $t - t_0 = T_{Opt} - \tau - t_0$ in the expression followed by θ_t.

with the constant m and each integrand being

$$m = 2\kappa\gamma/\sigma_v^2,$$

$$A_1'(\tau) = a^\theta\left(\beta + \mu z + z\frac{g'(z)}{g(z)}\right),$$

$$A_2'(\tau) = b^\theta\beta\cos\big(2\pi(T_{Opt} - \tau - t_0)\big),$$

$$A_3'(\tau) = b^\theta\mu\cos\big(2\pi(T_{Opt} - \tau - t_0)\big)z,$$

$$A_4'(\tau) = b^\theta\cos\big(2\pi(T_{Opt} - \tau - t_0)\big)z\frac{g'(z)}{g(z)},$$

(A.11)

the expressions followed by β, μ, z, $g(z)$ and $g'(z)$ can be found in Appendix B.1.

Equation (A.10) has a quasi-analytical solution which is given by[17]

$$A(\tau) = m\big(A_1(\tau) + A_2(\tau) + A_3(\tau) + A_4(\tau) + k_3\big).$$

(A.12)

The proof for $A_1(\tau)$ is in Sitzia (2018), $A_2(\tau)$ is direct and $A_3(\tau)$ is calculated using integration by parts[18]

$$A_1(\tau) = +a^\theta\left(\beta\tau - \frac{1}{\gamma}\big(\mu z + \ln g(z)\big)\right), \quad A_1(0) = -a^\theta\frac{\mu}{\gamma\omega},$$

$$A_2(\tau) = -b^\theta\frac{\beta y_\tau^s}{2\pi}, \qquad\qquad\qquad A_2(0) = -b^\theta\frac{\beta y_0^s}{2\pi},$$

$$A_3(\tau) = +b^\theta\frac{\mu z(\gamma y_\tau^c - 2\pi y_\tau^s)}{4\pi^2 + \gamma^2}, \qquad A_3(0) = +b^\theta\mu\frac{\gamma y_0^c - 2\pi y_0^s}{\omega(4\pi^2 + \gamma^2)}.$$

(A.13)

with y_τ^c, y_0^c, y_τ^s, y_0^s and m as in (2.28). Since $A_4'(\tau)$ is not integrable, we cannot directly obtain an analytic expression for $A_4(\tau)$ but, alternatively, we can approximate $A_4'(\tau)$ as a polynomial around $\tau = 0$ using a second order Taylor expansion.[19] We compute the integral of each polynomial and we get

$$A_{4,1}(\tau) = +b^\theta\frac{\tau}{\omega}y_0^c g'\big(\omega^{-1}\big), \qquad\qquad\qquad\qquad\qquad\qquad A_{4,1}(0) = 0,$$

$$A_{4,2}(\tau) = -b^\theta\frac{\tau^2}{2\omega}\left(g'\big(\omega^{-1}\big)\left(-2\pi y_0^s + \gamma y_0^c(1 + k_1 n_1 + k_2 n_2)\right) + \gamma y_0^c(k_1 n_3 + k_2 n_4)\right), \quad A_{4,1}(0) = 0,$$

$$A_4(\tau)\;\; = A_{4,1}(\tau) + A_{4,2}(\tau), \qquad\qquad\qquad\qquad\qquad\qquad\qquad A_4(0)\;\;\; = 0,$$

(A.14)

with n_1, n_2, n_3 and n_4 as in (2.29).

In particular, if the initial condition is $A(0) = 0$ and given (2.26), we have that

$$k_3 = -(A_1(0) + A_2(0) + A_3(0) + A_4(0)) = x_0 + x_0^s y_0^s + x_0^c y_0^c,$$

(A.15)

where

$$x_0 = a^\theta\frac{\mu}{\gamma\omega},$$

$$x_0^s = b^\theta\left(\frac{\beta}{2\pi} + \frac{2\pi\mu}{\omega(4\pi^2 + \gamma^2)}\right),$$

$$x_0^c = -b^\theta\frac{\mu\gamma}{\omega(4\pi^2 + \gamma^2)}.$$

(A.16)

---

[17] We say that it is quasi-analytical due to expression followed by the term $A_4(\tau)$.

[18] The proof is available by direct request to the authors.

[19] This closed-form expression is found thanks to Matlab's Symbolic Maths Toobox.

A.3 Proof of Proposition 3

With $B(\tau)$ as in Eq. (2.25) and θ_t following the multiple sinusoidal pattern defined in expression (2.6), Eq. (2.22) becomes (see footnote 16)

$$
\begin{aligned}
\frac{\partial A(\tau)}{\partial \tau} &= B(\tau)\kappa\left(a^\theta + b^\theta \cos\big(2\pi(T_{Opt} - \tau - t_0)\big) + c^\theta \sin\big(2\pi(T_{Opt} - \tau - t_0)\big)\right) \\
&= \frac{2\kappa\gamma}{\sigma_v^2}\left(\beta + \mu z + z\frac{g'(z)}{g(z)}\right)\left(a^\theta + b^\theta \cos\big(2\pi(T_{Opt} - \tau - t_0)\big) + c^\theta \sin\big(2\pi(T_{Opt} - \tau - t_0)\big)\right) \\
&= m\big(A_1'(\tau) + A_2'(\tau) + A_3'(\tau) + A_4'(\tau) + A_5'(\tau) + A_6'(\tau) + A_7'(\tau)\big),
\end{aligned} \tag{A.17}
$$

the expressions followed by β, μ, z, $g(z)$ and $g'(z)$ can be found in Appendix B.1, each integrand being

$$
\begin{aligned}
A_5'(\tau) &= c^\theta \sin\big(2\pi(T_{Opt} - \tau - t_0)\big)\beta, \\
A_6'(\tau) &= c^\theta \sin\big(2\pi(T_{Opt} - \tau - t_0)\big)\mu z, \\
A_7'(\tau) &= c^\theta \sin\big(2\pi(T_{Opt} - \tau - t_0)\big)z\frac{g'(z)}{g(z)}.
\end{aligned} \tag{A.18}
$$

Equation (A.17) has a quasi-analytical solution which is given by[20]

$$
A(\tau) = m\big(A_1(\tau) + A_2(\tau) + A_3(\tau) + A_4(\tau) + A_5(\tau) + A_6(\tau) + A_7(\tau) + k_3\big). \tag{A.19}
$$

The expressions followed by $A_1'(\tau)$-$A_4'(\tau)$ and $A_1(\tau)$-$A_4(\tau)$ are the same as in Appendix A.2, $A_5(\tau)$ is direct and $A_6(\tau)$ is calculated using integration by parts (see footnote 18)

$$
\begin{aligned}
A_5(\tau) &= c^\theta \frac{\beta y_\tau^c}{2\pi}, & A_5(0) &= c^\theta \frac{\beta y_0^c}{2\pi}, \\
A_6(\tau) &= c^\theta \frac{\mu z\big(2\pi y_\tau^s + \gamma y_\tau^c\big)}{4\pi^2 + \gamma^2}, & A_6(0) &= c^\theta \frac{\mu(2\pi y_0^c + \gamma y_0^s)}{\omega(4\pi^2 + \gamma^2)},
\end{aligned} \tag{A.20}
$$

with y_τ^c, y_0^c, y_τ^s, y_0^s and m as in expressions (2.28). Similarly to what occurred with $A_4'(\tau)$, $A_7'(\tau)$ is not integrable, and we approximate it using a second order Taylor expansion around $\tau = 0$ (see footnote 19). We compute the integral of each polynomial and we get the following expressions

$$
\begin{aligned}
A_{7,1}(\tau) &= +c^\theta \frac{\tau}{\omega} y_0^s g'\big(\omega^{-1}\big), & A_{7,1}(0) &= 0, \\
A_{7,2}(\tau) &= -c^\theta \frac{\tau^2}{2\omega}\Big(g'\big(\omega^{-1}\big)\big(2\pi y_0^c + \gamma y_0^s(1 + k_1 n_1 + k_2 n_2)\big) + \gamma y_0^s(k_1 n_3 + k_2 n_4)\Big), & A_{7,2}(0) &= 0, \\
A_7(\tau) &= A_{7,1}(\tau) + A_{7,2}(\tau), & A_7(0) &= 0,
\end{aligned} \tag{A.21}
$$

with n_1, n_2, n_3 and n_4 as in (2.29).

In particular, if the initial condition is $A(0) = 0$ and given (A.19), we have that

$$
\begin{aligned}
k_3 &= -(A_1(0) + A_2(0) + A_3(0) + A_4(0) + A_5(0) + A_6(0) + A_7(0)) \\
&= x_0 + x_0^s y_0^s + x_0^c y_0^c,
\end{aligned} \tag{A.22}
$$

---

[20] We say that it is quasi-analytical due to expressions followed by the terms $A_4(\tau)$ and $A_7(\tau)$.

where

$$x_0 = a^\theta \frac{\mu}{\gamma \omega},$$

$$x_0^s = -c^\theta \frac{\mu \gamma}{\omega(4\pi^2 + \gamma^2)} + b^\theta \left(\frac{\beta}{2\pi} + \frac{2\pi \mu}{\omega(4\pi^2 + \gamma^2)} \right),$$ (A.23)

$$x_0^c = -b^\theta \frac{\mu \gamma}{\omega(4\pi^2 + \gamma^2)} + c^\theta \left(\frac{\beta}{2\pi} + \frac{2\pi \mu}{\omega(4\pi^2 + \gamma^2)} \right),$$

and with $A_1(0)$-$A_4(0)$ as in Appendix A.2.

B Appendix for analytic expressions

B.1 Analytic expression for $B(\tau)$

Equation (2.23) has an analytical solution which is given by

$$B(\tau) = \frac{2\gamma}{\sigma_v^2} \left(\beta + \mu z + z \frac{g'(z)}{g(z)} \right),$$ (B.1)

where the function $g(z)$ is a linear combination of Kummer's (M) and Tricomi's (U) hypergeometric functions, whilst k_1 and k_2 are constants determined by the initial conditions of the differential equation

$$g(z) = k_1 M(a, b, z) + k_2 U(a, b, z),$$ (B.2)

$$g'(z) = \frac{a}{b} k_1 M(a+1, b+1, z) - a k_2 U(a+1, b+1, z),$$ (B.3)

with

$$a = -\left(\mu b + \beta c_1 \frac{\omega}{\gamma} + d_1 \frac{\omega}{\gamma^2} \right), \qquad \mu = -\frac{1}{2} \left(1 + \frac{c_1 \omega}{\gamma} \right),$$ (B.4)

$$b = 1 + 2\beta + \frac{c_0}{\gamma}, \qquad \beta = \frac{-c_0 \pm \sqrt{c_0^2 - 4d_0}}{2\gamma},$$ (B.5)

$$\omega = \pm \frac{\gamma}{\sqrt{c_1^2 - 4d_2}}, \qquad z = \frac{e^{-\gamma \tau}}{\omega}.$$ (B.6)

From the pair of possible values for β and ω, we choose $\pm = +$ for β and $\pm = -$ for ω.

In particular, if the initial condition is $B(0) = 0$, we have the following constants

$$k_1 = \frac{a \frac{U(a+1,b+1,\frac{1}{\omega})}{U(a,b,\frac{1}{\omega})} - \beta\omega - \mu}{\frac{a}{b} M(a+1, b+1, \frac{1}{\omega}) + a M(a, b, \frac{1}{\omega}) \frac{U(a+1,b+1,\frac{1}{\omega})}{U(a,b,\frac{1}{\omega})}},$$ (B.7)

$$k_2 = \frac{1 - k_1 M(a, b, \frac{1}{\omega})}{U(a, b, \frac{1}{\omega})}.$$ (B.8)

We apply the change of variable $B(\tau) = -\frac{y'(\tau)}{y(\tau)b_2}$ to equation (2.23) and we get

$$\left(\frac{y'(\tau)}{y(\tau)} \right)^2 \frac{1}{b_2} - \frac{y''(\tau)}{y(\tau)} \frac{1}{b_2} = b_0 + \frac{y'(\tau)}{y(\tau)} \frac{b_1}{b_2} + \left(\frac{y'(\tau)}{y(\tau)} \right)^2 \frac{1}{b_2},$$ (B.9)

which leads to the following homogeneous second order ODE with no constant coefficients

$$y''(\tau) - \left(c_0 + c_1 e^{-\gamma\tau}\right)y'(\tau) + \left(d_0 + d_1 e^{-\gamma\tau} + d_2 e^{-2\gamma\tau}\right)y(\tau) = 0. \qquad \text{(B.10)}$$

Conditional to the original (alternative) characterisation,[21] b_0, b_1 and b_2 are as in the left (right) column in expressions (2.24).[22] Conditional to the original set-up, the coefficients in $g(z)$ and $g'(z)$ are

$$
\begin{aligned}
c_0 &= -\kappa + iu\sigma_v\left(\sigma_S\rho_{Sv} + \rho_{yv}\frac{\alpha}{\gamma}\right), & d_0 &= -(u^2 + iu)\frac{q_2}{2}\left(\sigma_S^2 + \frac{\alpha^2}{\gamma^2} + 2\rho_{Sy}\sigma_S\frac{\alpha}{\gamma}\right), \\
c_1 &= -iu\sigma_v\rho_{yv}\frac{\alpha}{\gamma}e^{-\gamma(T-T_{Opt})}, & d_1 &= q_2(u^2 + iu)\frac{\alpha}{\gamma}\left(\frac{\alpha}{\gamma} + \rho_{Sy}\sigma_S\right)e^{-\gamma(T-T_{Opt})}, \\
& & d_2 &= -(u^2 + iu)\frac{q_2}{2}\frac{\alpha^2}{\gamma^2}e^{-2\gamma(T-T_{Opt})}.
\end{aligned}
$$

$$\text{(B.11)}$$

Alternatively, and conditional to the alternative set-up, the coefficients in $g(z)$ and $g'(z)$ are

$$
\begin{aligned}
c_0 &= -\kappa + iu\sigma_v\rho_{Fv}\frac{\alpha}{\gamma}, & d_0 &= -(u^2 + iu)\frac{q_2}{2}\frac{\alpha^2}{\gamma^2}, \\
c_1 &= -iu\sigma_v\rho_{Fv}\frac{\alpha}{\gamma}e^{-\gamma(T-T_{Opt})}, & d_1 &= q_2(u^2 + iu)\frac{\alpha^2}{\gamma^2}e^{-\gamma(T-T_{Opt})}, \\
& & d_2 &= -(u^2 + iu)\frac{q_2}{2}\frac{\alpha^2}{\gamma^2}e^{-2\gamma(T-T_{Opt})}.
\end{aligned}
\qquad \text{(B.12)}
$$

In the case of the original set-up, the proof is in Sitzia (2018). In the alternative set-up, we have followed the steps described in that work to obtain the correspondent expressions.[18]

B.2 Solutions to ST18 and ST21

For both models, the CF in expression (2.20) is given by the Fourier transform in equation (2.21). In ST18 and ST21, $B(\tau)$ solves the ODE in (2.23), with b_0, b_1 and b_2 as in expressions (2.24), right column (alternative set-up). Following the methodology described in Sitzia (2018), we apply the change of variable $B(\tau) = -\frac{y'(\tau)}{y(\tau)b_2}$ to equation (2.23), so that it becomes

$$\left(-\frac{y'(\tau)}{y(\tau)b_2}\right)' = b_0(\tau) + b_1(\tau)\left(-\frac{y'(\tau)}{y(\tau)b_2}\right) + b_2\left(-\frac{y'(\tau)}{y(\tau)b_2}\right)^2. \qquad \text{(B.13)}$$

Grouping constant parameters and exponentials, we get to the following second order ODE[23]

$$y''(\tau) - \left(c_0 + c_1(\tau)\alpha e^{-\lambda\tau}\right)y'(\tau) + c_2(\tau)\left(\alpha e^{-\lambda\tau}\right)^2 y(\tau) = 0, \qquad \text{(B.14)}$$

with coefficients

$$
\begin{aligned}
c_0 &= -\kappa, \\
c_1 &= -iu\sigma_v\rho_{Fv}\alpha e^{-\lambda(T-T_{Opt})}, \\
c_2 &= -\frac{\sigma_v^2(u^2 + iu)}{4}\left(\alpha e^{-\lambda(T-T_{Opt})}\right)^2.
\end{aligned}
\qquad \text{(B.15)}
$$

Now we apply a last substitution using some parameters ω, β and μ which will be determined in order to simplify the above equation into a confluent hypergeometric equation $g(z)$. These

---

[21] As defined in Sect. 2.1.2.

[22] Observe that the expression followed by b_2 is unconditional to the set-up.

[23] See that c_2 is d_2 in Sitzia (2018).

parameters are given by

$$\mu = -\frac{1}{2}\left(1 + \frac{c_1\omega}{\lambda}\right), \quad \beta = -\frac{c_0}{\lambda},$$
$$\omega = \frac{\gamma}{\sqrt{c_1^2 - 4d_2}}, \qquad z = \frac{e^{-\lambda\tau}}{\omega}. \tag{B.16}$$

The function $g(z)$ is a linear combination of Kummer's (M) and Tricomi's (U) hypergeometric functions

$$g(z) = k_1 M(a, b, z) + k_2 U(a, b, z), \tag{B.17}$$
$$g'(z) = \frac{a}{b} k_1 M(a+1, b+1, z) - a k_2 U(a+1, b+1, z), \tag{B.18}$$

with parameters

$$a = -\mu b + \omega \frac{c_0 c_1}{2\lambda}, \qquad\qquad b = 1 - \beta. \tag{B.19}$$

The expressions followed by k_1, k_2 and $B(\tau)$ are the same as in TS09-SV1 and our model, they can be found in Appendix B.1. In ST18, $A(\tau)$ solves the same ODE as in TS09-SV1. The integral is direct, its analytical solution and k_3 are given by equations (2.34). In ST21, $A(\tau)$ solves the same ODE (2.22) as in our model. While $A(\tau)$ depends on the specification of θ_t, in this work we only focus on their sinusoidal pattern, defined in equation (2.5). The integral of $A(\tau)$ is not direct any more. We provide it in Proposition 2 with proof in Appendix A.2.

References

Arismendi, J. C., Back, J., Prokopczuk, M., Paschke, R., & Rudolf, M. (2016). Seasonal stochastic volatility: Implications for the pricing of commodity options. *Journal of Banking and Finance, 66*, 53–65.

Back, J., Prokopczuk, M., Paschke, R., & Rudolf, M. (2013). Seasonality and the valuation of commodity options. *Journal of Banking and Finance, 37*, 273–290.

Bates, D. S. (1996). Jumps and stochastic volatility: Exchange rate processes implicit in deutsche mark options. *Review of Financial Studies, 9*(1), 69–107.

Baum, C. F., Zerilli, P., & Chen, L. (2021). Stochastic volatility, jumps and leverage in energy and stock markets: Evidence from high frequency data. *Energy Economics, 93*, 104481.

Benth, F. E., & Vos, L. (2013). Cross commodity spot price modeling with stochastic volatility and leverage for energy markets. *Advances in Applied Probability, 45*(2), 545–571.

Black, F. (1976). The pricing of commodity contracts. *Journal of Financial Economics, 3*(1), 167–179.

Black, F., & Scholes, M. (1973). The pricing of options and corporate liabilities. *Journal of Political Economy, 81*(3), 637–654.

Brix, A. F., Lunde, A., & Wei, W. (2018). A generalized Schwartz model for energy spot prices: Estimation using a particle MCMC method. *Energy Economics, 72*, 560–582.

Carr, P., & Madan, D. B. (1999). Option valuation using the fast Fourier transform. *Journal of Computational Finance, 2*(4), 61–73.

Chiarella, C., Kang, B., & Nikitopoulos, C. (2013). Humps in the volatility structure of the crude oil futures market: New evidence. *Energy Economics, 40*, 989–1000.

Clewlow, L., & Strickland, C. (1999). *Valuing energy options in a one factor model fitted to forward prices, Research Paper Series 10*. Quantitative Finance Research, Centre University of Technology.

Clewlow, L., & Strickland, C. (1999). *A multi-factor model for energy derivatives, Research Paper Series 28*. Quantitative Finance Research Centre, University of Technology.

Clewlow, L., & Strickland, C. (2000). *Energy Derivatives: Pricing and Risk Management*. Lacima Publications.

Collin-Dufresne, P. & Goldstein, R. S. (2002). Generalizing the affine framework to HJM and random field models. https://ssrn.com/abstract=410421

Cox, J. C., Ingersoll, J. E., & Ross, S. A. (1985). A theory of the term structure of interest rates. *Econometrica, 53*(2), 385–407.

Crosby, J., & Frau, C. (2022). Jumps in commodity prices: New approaches for pricing plain vanilla options. *Energy Economics, 14*, 106302.

Duffie, D. (2001). *Dynamic asset pricing theory*. Princeton University Press.

Duffie, D., Pan, J., & Singleton, K. (2000). Transform analysis and asset pricing for affine jump-diffusions. *Econometrica, 68*, 1343–1376.

Eydeland, A., & Geman, H. (1998). Pricing power derivatives. *Risk* (October), 53–60.

Fanelli, V. (2020). *Financial modelling in commodity markets*. Chapman & Hall/CRC Press.

Fanelli, V., Maddalena, L., & Musti, S. (2016). Modelling electricity futures prices using seasonal path-dependent volatility. *Applied Energy, 173*, 92–102.

Fanelli, V., & Schmeck, M. D. (2019). On the seasonality in the implied volatility of electricity options. *Quantitative Finance, 19*(8), 1321–1337.

Geman, H. (2000). Scarcity and price volatility in oil markets. *EDF Trading Technical Report*.

Geman, H., & Nguyen, V.-N. (2005). Soybean inventory and forward curve dynamics. *Management Science, 51*(7), 1015–1164.

Heath, D., Jarrow, R., & Morton, A. (1992). Bond pricing and the term structure of interest rates: A new methodology for contingent claims valuation. *Econometrica, 60*(1), 77–105.

Heston, S. L. (1993). A closed-form solution for options with stochastic volatility with applications to bond and currency options. *Review of Financial Studies, 6*(2), 327–343.

Hylleberg, S. (Ed.). (1992). *Modelling seasonality*. Oxford University Press.

Jana, R., & Gosh, I. (2022). A residual-driven ensemble machine learning approach for forecasting natural gas prices: Analyses for pre- and during COVID-19 phases. *Annals of Operations Research*. https://doi.org/10.1007/s10479-021-04492-4

Jotanovic, V., & D'Ecclesia, R. L. (2021). The European gas market: New evidences. *Annals of Operations Research, 299*, 963–999.

Kristoufek, L. (2014). Leverage effect in energy futures. *Energy Economics, 45*, 1–9.

Lucia, J. J., & Schwartz, E. (2002). Electricity prices and power derivatives: Evidence from the Nordic power exchange. *Review of Derivatives Research, 5*(1), 5–50.

Merton, R. (1976). Option pricing when underlying stock returns are discontinuous. *Journal of Financial Economics, 3*(1–2), 125–144.

Nomikos, N., & Andriosopoulos, K. (2012). Modelling energy spot prices: Empirical evidence from NYMEX. *Energy Economics, 34*, 1153–1169.

Richter, M. & Sørensen, C. (2002). *Stochastic volatility and seasonality in commodity futures and options: The case of soybeans*. Working Paper 4, Copenhagen Business School, Department of Finance. http://ssrn.com/abstract=301994

Rogel-Salazar, J., & Sapsford, N. (2014). Seasonal effects in natural gas prices and the impact of the economic recession. *Wilmott Magazine, 74*, 74–81.

Samuelson, P. A. (1965). Proof that properly anticipated prices fluctuate randomly. *Industrial Management Review, 6*(2), 41–49.

Santangelo, A. (2017). *Pricing of gas storage contracts using a temperature dependent gas price model*. PhD. thesis, University of Milan-Bicocca.

Schmelzle, M. (2010). *Option pricing formulae using Fourier transform: Theory and application*. https://pfadintegral.com/docs/Schmelzle2010%20Fourier%20Pricing.pdf

Schneider, L., & Tavin, B. (2018). From the Samuelson volatility effect to a Samuelson correlation effect: An analysis of crude oil calendar spread options. *Journal of Banking and Finance, 95*, 185–202.

Schneider, L., & Tavin, B. (2021). Seasonal volatility in agricultural markets: Modelling and empirical investigations. *Annals of Operations Research*. https://doi.org/10.1007/s10479-021-04241-7

Sitzia, N. (2018). *The analytical solution of Trolle–Schwartz model*. MSc. thesis, École Polytechnique Fédérale de Lausanne'. https://ssrn.com/abstract=3121906

Sørensen, C. (2002). Modeling seasonality in agricultural commodity futures. *The Journal of Futures Markets, 22*(5), 394–426.

Trolle, A. B., & Schwartz, E. S. (2009). Unspanned stochastic volatility and the pricing of commodity derivatives. *Review of Financial Studies, 22*(11), 4423–4461.